Quantifying particle motion under force fields in microfluidic systems by image tracking methods

A Thesis

Presented to

the faculty of the School of Engineering and Applied Science

University of Virginia

in partial fulfillment

of the requirements for the degree

Master of Science

by

Name

Andrew Chen

Month degree is awarded   August

Year   2016

APPROVAL SHEET

The thesis

is submitted in partial fulfillment of the requirements

for the degree of

Master of Science

andrew Chen

AUTHOR   *signature*

The thesis has been read and approved by the examining committee:

Please insert committee member names below:

Nathan Swami

Advisor

Stephen G. Wilson

Daniel S. Weller

Accepted for the School of Engineering and Applied Science:

Craig H. Benson, Dean, School of Engineering and Applied Science

Month degree is awarded

August

Year   2016

Print Form

Abstract

Micro-engineered devices for selective cell separation and analysis are of great importance in biomedical research. Dielectrophoresis (DEP), which enables the frequency-selective translation of particles under spatially non-uniform fields based on their distinctive impedance characteristics, is an effective technique for cell sorting and quantification. It has been used for selective manipulation and identification of microorganisms and cells. Particle translation towards or away from localized regions of high field occurs, respectively, under positive DEP (p-DEP) or negative DEP (n-DEP). In this manner, based on differences in polarization between different cells and the surrounding medium, non-destructive and label-free cell separations can be accomplished. This work is focused on using image analysis methods to quantify the translation of particles under spatially non-uniform fields to determine the DEP force spectrum versus frequency, within two different device designs. The first is based on a constricted microfluidic channel, wherein image tracking is used to directly identify particle translation, to quantify the DEP frequency spectra with single-particle sensitivity. The second is a set of microfluidic wells with ring electrodes, wherein the focus is on rapid quantification of DEP spectra, based on spatio-temporal analysis of light scattering due to particle translation.

These techniques are applied to three kinds of bioparticles, *Cryptosporidium parvum*, *Clostridium difficile* and Human Embryonic Kidney (HEK) cell as subjects to validate a model for particles of different sizes and shapes.

These methods could serve as useful tools to study cellular subpopulations, which is of fundamental importance in biomedical sciences.

Content

3

Chapter 1

Introduction

In recent decades, different methods, such as optical, microfluidic, mechanical and electrical fields are developed to control micro-/nano-particles. These techniques have been widely applied in trapping, characterizing and separating particles[1].Using electrical fields is very suitable for the precise control of bioparticles like bacteria[2], yeast, apoptosis, viruses, proteins[3] and DNA due to some advantages of good controllability, easy operation, high efficiency and small damage to the particles[1].

Electrophoresis and dielectrophoresis are two main electrokinetic manipulations of particles translations in electrical fields[4]. Electrophoresis is a phenomenon that causes particles to be charged and moved along the electric field lines. But it is very difficult to distinguish particles have similar electrophoretic mobilities in electrical fields or particles which cannot be charged effectively. Unlike electrophoresis, dielectrophoresis does not require particles to be charged and can overcome these problems[5].

1.1 Introduction to Dielectrophoresis

Dielectrophoresis is the motion of a dielectric particle when it is subjected to a non-uniform electric field. The strength and direction of DEP force are depending on the shape and size of particles, the electrical properties of medium and particles, and the frequency and distribution of electric field. This frequency-selective translation of polarized particles is widely investigated for manipulation and analysis of micro-organisms [6][7]. In the presence of phase difference in the system of electrodes, moving electric field will cause planar movement of particles parallel to electrodes which is called traveling wave dielectrophoresis (twDEP)[8] or rotation of particles under rotating electric field which is electrorotation (ROT) [9]. These two phenomena are special cases of DEP.

1.2 Polarization and Clausius-Mossotti Factor

Polarization is the main factor for dielectrophoresis to drive the dielectric material particles. Then dipole moment was induced and dipoles were produced [4]. The

distribution of charges to produce the electrical dipole includes two charges of the same magnitude and opposite sign, separated by a distance d. The dipole moment of the vector **P** directed from the negative to the positive charge is presented as

$$P = Qd \tag{1.1}$$

Q is the charge and d is the distance of separation two charges. Under a non-uniform electrical field, the dipole moment is induced and results in DEP force exerted on particles.

The DEP force is expressed as follows:

$$F_{DEP} = (P \cdot \nabla)E \tag{1.2}$$

E is the electric field and this equation shows that a field non-uniformity (∇E) is required for a non-zero DEP force.

The magnitude of the polarizability and the effective dipole moment of the particle, all depend on the frequency. The function of the dependence for spherical particles is expressed as follows:

$$f_{CM} = \frac{\varepsilon_p^* - \varepsilon_m^*}{\varepsilon_p^* + 2\varepsilon_m^*} \tag{1.3}$$

$$\varepsilon_p^* = \varepsilon_p - \frac{\sigma_p}{j\omega} \qquad \varepsilon_m^* = \varepsilon_m - \frac{\sigma_m}{j\omega} \tag{1.4}$$

σ_p and σ_m are the conductivity of the particle and surrounding medium. ε_p and ε_m are the permittivities of the particle and surrounding medium. f_{CM} is called the Clausius-Mossotti factor and is the measure of particle polarizability.

For a typical spherical particle, the change of the magnitude of the force is produced by the real part of the Clausius-Mossotti factor [10]. Considering the effective polarizability of a spherical particle, the time-averaged DEP force is expressed as follows:

$$F_{dep} = 2\pi a^3 \varepsilon_m Re(f_{CM}) \nabla |E^2| \tag{1.5}$$

For ellipsoid particles with the major axis l and minor axis r, the Clausius-Mossotti factor is [5]:

$$f_{CM} = \frac{\varepsilon_p^* - \varepsilon_m^*}{\varepsilon_m^* + (\varepsilon_p^* - \varepsilon_m^*)L} \tag{1.6}$$

Where $L = \frac{r^2}{2l^2}\left[ln\left(\frac{1-e}{1+e}\right) - 2e\right], e = \sqrt{1 - \frac{r^2}{2l^2}}$

The time-averaged DEP force for ellipsoid particles is expressed as follows [11]:

$$F_{dep} = \frac{\pi l r^2}{6}\varepsilon_m Re(f_{CM})\nabla|E^2| \tag{1.7}$$

The factors affecting the magnitude of the force are the minor axis (r) and the major axis (l) of ellipsoid particles, the permittivity of the suspending medium (ε_m) and the gradient of the square of the field strength ($\nabla|E^2|$). The effects of frequency and direction of the force on F_{dep} are defined by the real part of the Clausius-Mossotti factor.

If the polarizability of the particle is larger than that of the suspending medium, Positive DEP (p-DEP) was found, that is $Re(f_{CM}) > 0$, and bio-particles are driven to the high electric field strength by positive DEP. If the polarizability of the particle is lower than that of the suspending medium, Negative DEP (n-DEP) was found, that is $Re(f_{CM}) < 0$, bio-particles are driven to the low field strength by negative DEP [11].

The numeric value of $Re(f_{CM})$ was determined by the terms of $(\sigma_p - \sigma_m)$ or $(\varepsilon_p - \varepsilon_m)$[11]. The effect of the electric field could be evaluated by the change of its frequencies. At low frequencies, the conductivity of the particle and suspending medium is the main factor. The real part of the Clausius-Mossotti factor are expressed as $\frac{\sigma_p-\sigma_m}{\sigma_p+2\sigma_m}$ for spherical particles and $\frac{\sigma_p-\sigma_m}{\sigma_m+(\sigma_p-\sigma_m)L}$ for elliptic particles. At middle frequencies, the numeric values of $\sigma_p - \sigma_m$ and $\varepsilon_p - \varepsilon_m$ need to be considered. At high frequencies, the permittivity of the particle and suspending medium is dominated. The real part of the Clausius-Mossotti factor is expressed as $\frac{\varepsilon_p-\varepsilon_m}{\varepsilon_p+2\varepsilon_m}$ for spheral particles and $\frac{\varepsilon_p-\varepsilon_m}{\varepsilon_m+(\varepsilon_p-\varepsilon_m)L}$ for elliptic particles.

From the above discussion, the factors affecting p-DEP and n-DEP are the frequencies of AC field, conductivity and permittivity of bio-particles and suspending medium.
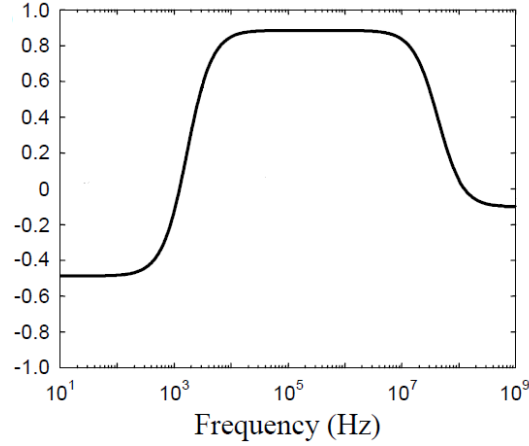
Figure 1. Variation of the real part Clausius-Mossotti factor with frequency for a particle to simulate a cell with a conductive core and an insulating shell [11]

The variation of the real part of Clausius-Mossotti factor with frequency is shown in Figure 1. If the conductivity and permittivity of particle and surrounding medium at different frequencies are found, the relationship between the real CM factor and frequency could be plotted. When the CM factor equals to zero, the frequency is called crossover frequency. The magnitude of DEP force is zero in this situation.

By measuring and quantifying DEP force at different frequencies, the dispersion spectra of the real CM factor versus frequency can be plotted. The conductivity and permittivity of the particle can be calculated. The real CM factor based on the dielectrophoretic characteristics can then be used to monitor alterations in particle properties after various treatments, such as the effect of antibiotics and silver nanoparticles [12]. This technique can be used for the discrimination of particles or for comparison of the effects of different treatments [13][14].

1.3 Research Motivation

From equations (1.5) and (1.7), DEP force is relative to the particles' size and shape, the electric field frequency, and the gradient of the square of the field strength. The measurements of the quantifying of DEP force have some challenges because of the differences of particles' size and shape, especially the magnitude of electric field. DEP force exerted on the particle is not a constant because the strength of non-uniform electric

field changes with a position of a particle in a device. The real CM factor of a particle is expressed follows

$$Re(f_{CM}) = \frac{F_{dep}}{K\varepsilon_m \nabla|E^2|} \tag{1.8}$$

Where K is a constant of size and shape of a particle and ε_m is a permittivity of a medium.

With the unchanged $Re(f_{CM})$ in a fixed frequency , in the region of the microfluidic devices to measure DEP force, the magnitude of F_{dep} changes abruptly with a slight distance of particle movement such as a few micrometers. Moreover, different sizes of the same type of particle cause the force different as well. From both reasons, it is very hard to define the reference position to measure DEP force in a fair standard and cause the inaccurate result of measuring DEP force spectrum which is considered the relative value of $Re(f_{CM})$ with frequency. A more accurate analysis of measured result should be developed to transfer the inconstant DEP force into a reliable computation based on a fair basis. To overcome this challenge, normalization is a way to eliminate the effects of electric field [15] and particles' size.

If the DEP force could be normalized by $\nabla|E^2|$ in different position and size of a particle, equation (1.8) can be rewritten as:

$$Normalized\ F_{dep} = G\ Re(f_{CM}) \tag{1.9}$$

Where G is a constant relative to the shape of particle and the magnitude of ε_m. In the condition of the fixed frequency and medium, G is unchanged .If the value of $Re(f_{CM})$ of particles are the same, it means that the polarizabilities of these particles are the same. Therefore, the same type of particles should have the same constant normalized DEP force even their size or position are different. This method is expected to apply a fair basis to compare the normalized DEP force between different particles and calculate a constant normalized DEP force of a specific particle in the various position.

Hence, the main objective of this thesis is to develop methodologies which are able to measure the normalized dep force exerted on different bioparticles with different frequencies to improve the accuracy of computing the electrophysiology properties of bioparticles from the DEP force spectrum.

1.4 Quantifying DEP Force

Many techniques are developed to quantify the dielectrophoretic response. Because it is impossible to directly measure the force on a particle, several indirect measurement techniques are developed such as the collection of a number of particles, the detection of the speed of motion or the levitation height [16].

However, these measurements do not calculate the absolute DEP force on the particle, they only provide a proportional strength and direction of the force on the particles to construct the model spectrum which the Clausius–Mossotti factor of a particle is considered for. In this thesis, two kinds of quantifications are applied to measure DEP force on a single bioparticle and a bioparticle population.

1.4.1 Quantifying DEP force on bioparticles by velocity tracking measurements

Measuring the velocity and direction of the motion of a particle is the way to quantify DEP force for the individual particle. If a particle is moving in the fluid, a viscous drag force is produced by the action of the fluid on the particle. The force is related to and acts against the velocity.

$$F_\eta = -fv \tag{1.10}$$

The constant f is called the friction factor and related to the particle properties, such as size, shape, and surface. For a sphere particle,

$$f = 6\pi\eta a \tag{1.11}.$$

For an ellipsoid particle, if the movement of particle is parallel to the l direction,

$$f = \frac{8\pi\eta l}{2\ln(2l/r)-1} \tag{1.12}$$

where η is the viscosity of the medium, a is the radius of a sphere, l is the major axis of ellipsoid and r is the minor axis of the ellipsoid.

When a particle in a fluid is experiencing deterministic force, the drag force increases. If the acting force is constant, the article will reach a terminal velocity. If the fluid is moving, the terminal velocity of this particle is affected by the fluid velocity. By the Newton's second law, the motion equation of the particle is expressed as follow:

$$F = m\frac{dv}{dt} \tag{1.13}$$

9

where F is the total force acting on the particle, m is the mass of the particle and v is the velocity of the particle.

If the Brownian motion and the buoyancy force are ignored, the movement of a particle due to a DEP force is expressed as follow [11]:

$$m\frac{dv}{dt} = F_{DEP} - F_{\eta} \tag{1.14}$$

where F_{DEP} is the DEP force and F_{η} is the viscous force.

This equation can be determined by tracking displacement (x) as a function of time (t) as follows [13]:

$$F_{DEP} = m\frac{d^2x}{dt^2} + f\frac{dx}{dt} \tag{1.15}$$

If the shape and radius of particle and tracking which moving with time are known, the DEP force in different positions can be quantified individually.

1.4.2 Quantify the spatio-temporal changing of the force field

The collection rate measurement is another common method to quantify the DEP force for the bioparticles such as cell, bacteria, and algae [16]. Detecting electrodes are immersed into the solutions with predetermination concentration of particles. After a fixed period of time, the particles collected at the electrode are counted by simple counting method or by measuring the fluorescence near the electrode edge for fluorescent particles [16].

To quantify the DEP force in the collection region, the change rate in fluorescence intensity (I) is proportional to the rate of change in a number of particles entering that particular region (n) and the change rate of particle concentration (c) in the region imaged by the pixel. Assuming a uniform initial particle concentration in the pre-concentration region. The relationship could be described by the Fokker-Planck equation (FPE) and expressed by follows:

$$\dot{I} \propto \frac{\partial n}{\partial t} \propto \frac{\partial c}{\partial t} = -\nabla \cdot J_{Total} \tag{1.16}$$

where J_{Total} is the total flux of particles due to the net force field.

If the interactions between particle and particle are neglected, the total particle flux J is the summation of particle fluxes caused by each force:[17]

$$J_{Total} = J_{DEP} + J_{Diffusion} \qquad (1.17)$$

The relation of the concentration of particles $c = c(r,t), r = x, y, z$ and the particle flux J is expressed as follows:

$$\frac{\partial c}{\partial t} = -\nabla \cdot J = -\frac{1}{f}\nabla \cdot \left(c\frac{\alpha(\omega)}{2}\nabla |E^2| \right) + \nabla \cdot D\nabla c \qquad (1.18)$$

where α is the function that the real part of the frequency (ω) depend on effective polarizability of the particle under DEP. For a spherical particle, $\alpha = 4\pi r^3 \varepsilon_m Re\{f_{CM}\}$, for an ellipsoid particle, $\alpha = \frac{\pi l r^2}{3}\varepsilon_m Re(f_{CM})\nabla E^2$, E is the RMS value of an electric field, ∇ is the gradient operator, $D = \frac{k_B T}{f}$ is the diffusion constant, and f is the particle friction factor.

Combining above equations, the rate of change in florescent intensity ($\dot{I}$) is as follows:

$$\dot{I} \propto -\nabla \cdot J = -\frac{1}{f}\nabla \cdot \left(c\frac{\alpha(\omega_1)}{2}\nabla |E^2| \right) + \nabla \cdot D\nabla c \qquad (1.19)$$

From the above equation of the rate of change in florescence intensity, two conditions are simplified. The particle polarizability is the only significant parameter that causes the DEP force which dominates in the net flux in the collection region (only in early times). Thus, the flux of diffusional force can be neglected because it is much smaller than the flux of DEP force in the region close to the electrodes. The DEP force dispersion is then calculated by the variation of force field at various frequencies. Therefore, the rate of change in florescence intensity of a pixel in the concentration region under a predetermined DEP force field at two frequency ω_1 and ω_2 is the ratio of the relative DEP forces on the particle at these frequencies. The ratio of the quantitative computation of force dispersion is as follows:

$$\frac{\dot{I}(\omega_1)}{\dot{I}(\omega_2)} = \frac{F_{dep}(\omega_1)}{F_{dep}(\omega_2)} = \frac{\frac{1}{f}\left(c\frac{\alpha(\omega_1)}{2}\nabla |E^2| \right)}{\frac{1}{f}\left(c\frac{\alpha(\omega_2)}{2}\nabla |E^2| \right)} \qquad (1.20)$$

The ration can be used to describe the relative polarization ability of particles in different frequencies. By plotting the relative DEP force spectrum of particles, the real CM factor which is the particle characteristic can be described.

1.5 Three Subjects of Bioparticles

Three kinds of micrometer-size bioparticles of different sizes and shapes are as subjects in the thesis.

1.5.1. *Cryptosporidium parvum*

Cryptosporidium parvum is a protozoan parasite and cause cryptosporidiosis which is a parasitic disease of the mammalian intestinal tract. It produces oocysts at its infective stage in life cycle. If the parasite is present in the body, their oocysts in fecal samples would be indicated. This parasite is waterborne and also found to infect livestock [18]. Since infection can be caused by just a few oocysts, its detection is difficult due to the need for high sensitivities.

1.5.2. *Clostridium difficile*

The shape of *Clostridium difficile* appears like a long, irregular, spindle-shaped cell. The *C. difficile* cells are Gram-positive and grow optimal on blood agar at human body temperatures in the absence of oxygen. The bacteria produce spores under stress so it can tolerate extreme conditions that the other active bacteria cannot survive within. Recently, they have been identified as a serious threat to global public health [19].

1.5.3. Human Embryonic Kidney (HEK) cell

This cell line originally derived from human embryonic kidney cells grown in tissue culture. Because of the ease for growth and transfection, they are widely used in cell biology research and used as hosts for gene expression. This type of cells can be used to produce antibodies to study pharmacokinetics and glycosylation [20]

The size and shape of these cells are different. *Clostridium difficile* is an ellipsoid, the general minor axis of it is 500nm and major axis is 3um. *Cryptosporidium parvum* and Human Embryonic Kidney (HEK) cells are spheres and their radii are 4-6um and 11-20um, respectively.

Different DEP techniques are applied to these three kinds of micrometer-size bioparticles as subjects to characterize their electrophysiology.
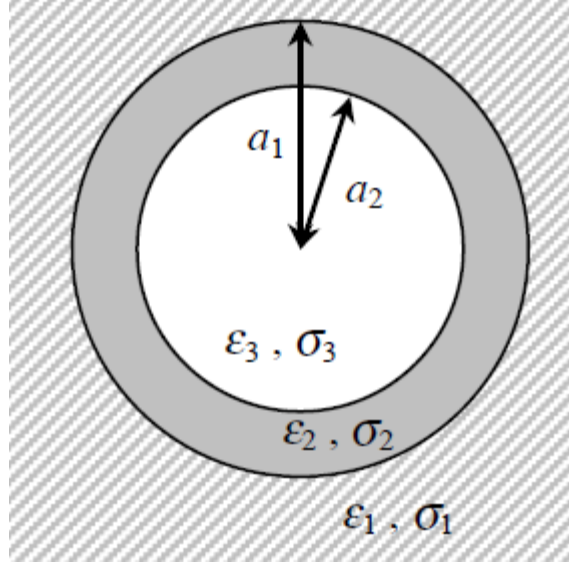
1.6 Shell Models

Figure 2 Schematic of a particle with a single shell [11]

The electrophysiology properties of bioarticles can be calculated by the real CM factor of a cell model .Cells usually have a complicated internal structure. The simplest model to express the structure is a single shelled particle as shown schematically in figure 2.The model assigns different electrical properties to the core (cytoplasm) and the shell (membrane) of the bioparticle. σ_1, σ_2 and σ_3 are the conductivity of the surrounding medium, membrane ,and cytoplasm ,respectively. ε_1 , ε_2 and ε_3 are the permittivities of the surrounding medium, membrane ,and cytoplasm ,respectively. a_1 is a radius of a cell and a_2 is a radius of cytoplasm.

1.6.1 Single Shell Models for a spherical particle[11]

The f_{CM} of spherical particle with single shell is given by the respective complex permittivity values ,as follows:

$$f_{CM,23} = \frac{\varepsilon_{23}^* - \varepsilon_1^*}{\varepsilon_{23}^* + 2\varepsilon_1^*} \tag{1.21}$$

Where $\varepsilon_{23}^* = \varepsilon_2^* \cdot \left[\left(\frac{a_2}{a_1}\right)^3 + 2\left(\frac{\varepsilon_3^* - \varepsilon_2^*}{\varepsilon_3^* + 2\varepsilon_2^*}\right)\right] \Big/ \left[\left(\frac{a_2}{a_1}\right)^3 - \left(\frac{\varepsilon_3^* - \varepsilon_2^*}{\varepsilon_3^* + 2\varepsilon_2^*}\right)\right]$

The representation of (1.) is equivalent to a homogeneous spherical particle of radius a_1 and permittivity ε_{23}^* .The effective polarisability of a single shell spherical particle can

be described by the $f_{CM,23}$. In the thesis, particles of *Cryptosporidium parvum* and HEK cell can use the model to express their CM factor and calculate their electrophysiology properties.

1.6.2 Single Shell Models for an ellipsoid particle [21]

The f_{CM} of ellipsoid particle with single shell is given by the respective complex permittivity values ,as follows:

$$f_{CM,single\ shell\ ellipsoid} = \frac{\varepsilon_3^* - \varepsilon_1^*}{3[\varepsilon_1^* + L_1(\varepsilon_2^* - \varepsilon_1^*)] + 9K\frac{r_2^2 l_2}{r_1^2 l_1}L_1(1 - L_1)(\varepsilon_2^* - \varepsilon_1^*)} \tag{1.22}$$

Where $K = \frac{\varepsilon_3^* - \varepsilon_2^*}{3[\varepsilon_2^* + L_1(\varepsilon_3^* - \varepsilon_2^*)]}$, $L_1 = \frac{r_1^2}{2l_1^2 e_1^3}\left[\ln\left(\frac{1+e_1}{1-e_1}\right) - 2e_1\right], e_1 = \sqrt{1 - \frac{r_1^2}{l_1^2}}$, r_1 and r_2 are the length of cell and cytoplasm ,respectively, a_1 and a_2 is the radius of cell and cytoplasm ,respectively.

The magnitude of $f_{CM,single\ shell\ ellipsoid}$ is greatly relative to the radius and length of an ellipsoid particle. Thus, the magnitude of the CM factor of different ellipsoid particles are different apparently because of their size differences. In the thesis, the structure of *Clostridium difficile* can be described by this model.

1.7 Thesis Outline

Aiming at developments of two methodologies for measuring and normalizing DEP force of multiple bioparticles, the thesis is outlined as follows:

Chapter 1 first introduces the rationale of DEP force and CM factor which can characterize bioparticles by their properties of electrophysiology. Then we discuss the quantification of DEP force and the necessary of the normalization for measuring DEP force spectrum. Finally, we compare three different bioparticles and their shell models.

Chapter 2 provides the methodology to quantify the DEP force on observable individual particles with different sizes and shapes by tracking their velocities in different positions at a constriction chip. Then develops the normalization of their DEP force for the different sizes and a different magnitude of electric field at various positions.

Chapter 3 discusses another methodology to quantify the DEP force on particle population and find a suitable measuring region for normalizing DEP force in DEP wells. Chapter 4 concludes the entire thesis and discusses future work.

Chapter 2

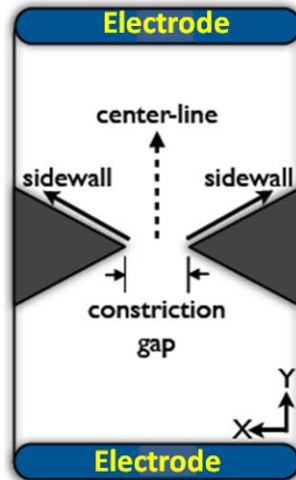## Velocity Tracking Measurements

2.1 Constriction Chip

Figure 3. The diagram of the constriction chip[13]

A constriction chip can be used to track the movement and measure the velocity of an individual particle. The positions of the electrodes are at the inlet and outlet of the device and the location to observe the movement of individual particles is at the region near both tips of insulating constrictions. The higher electric field is produced by insulating constrictions between the electrodes.

The triangular constrictions of an insulating material are used to manipulate the electric field [22]. The local field enhancement can be explained by the electric current density equation,

$$J = \sigma E \tag{2.1}$$

where J is the current density, σ is conductivity of the electrolyte medium, and E is the electric field.

If the constriction is perfectly insulating, the current carrying ions are only forced through a narrower path, and the current density will only increase along the constricted areas. So the increase of the current density increases the electric field at these points. [22]

Figure 4 illustrates the electric field lines which are scattered away from insulator in a parallel direction and these lines are bent and concentrated at the constriction tip of the insulating material.
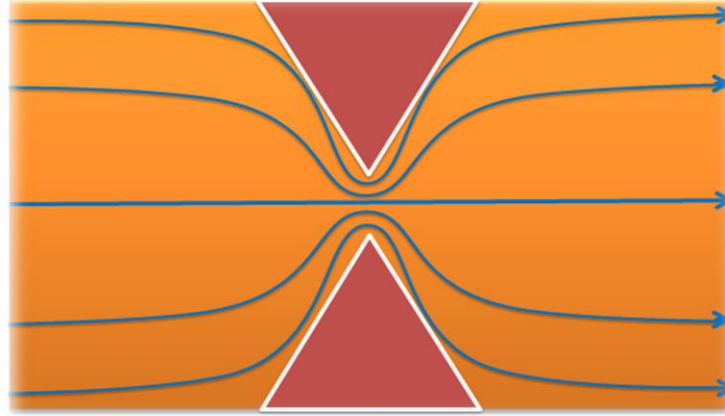

Figure 4. The illustration of the electric field lines

The dimensions of the constriction affect the field gradient and the magnitude at constriction area. So the high field point is located at the tips of the constriction. That is, the region has the highest concentration of electric field. The magnitude of this high field point depends on the magnitude of the applied electric field and the gap size of the constrictions.

The gap size and the shape of insulators affect the distribution of electric field as well. With decreasing gap size, the electric current density increases because of a number of electric field lines do not change but they get concentrated in the decreased gap. Thus, the concentrated of the electric field also increases by equation (1.1). Obviously, the sharpness or slopes of the constriction determine the gradient of the applied field. The sharper the tip of the insulators, the steeper the field gradient is. [22]

The motion of different micrometer-sized cells can be measured by this chip. When particles approach the region near tips, stronger P-DEP force adsorbs them on the tips. On the contrary, N-DEP pushes particles away from tips. By equation (1.15), their DEP force at different positions can be quantified by their expression of cell moving.
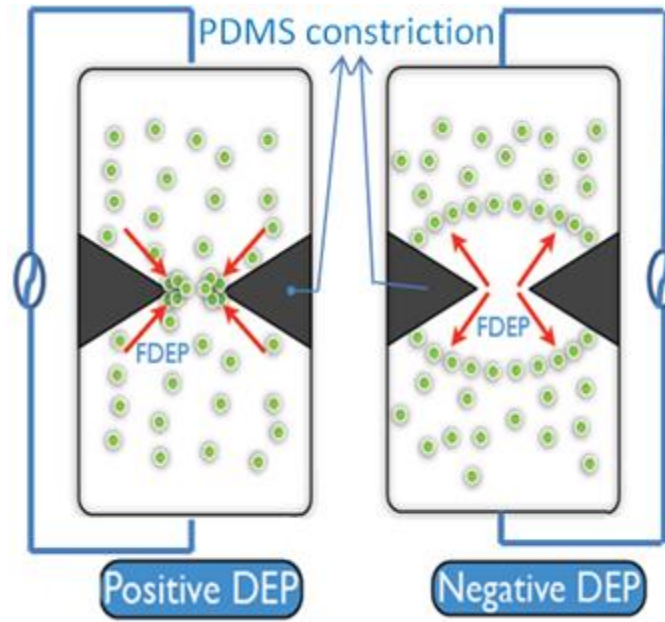
Figure 5- PDEP and NDEP force in a structure of constriction chip [13]

The electrical field lines are bent at the triangle insulator, thereby producing high field points at the tip of the insulator constriction, while the low field region is localized right before the constriction. Hence, pDEP causes particles to be driven to the high field points; i.e. constriction tip, while nDEP causes particles to be driven away from the high field points, as shown in Figure 5. It is note that the intensity distribution of field is symmetrical along the center lines.

The highest intensity was found in the region between two tips of constrictions. The DEP force decreased when the distance from the center position of two tips increases. The closer the position of a particle to center, the stronger of DEP force is. By equation (1.15), with the tracking of the particle's route and finding the moving distance of individual particle, the velocity and acceleration can be calculated and then the DEP force can be quantified.
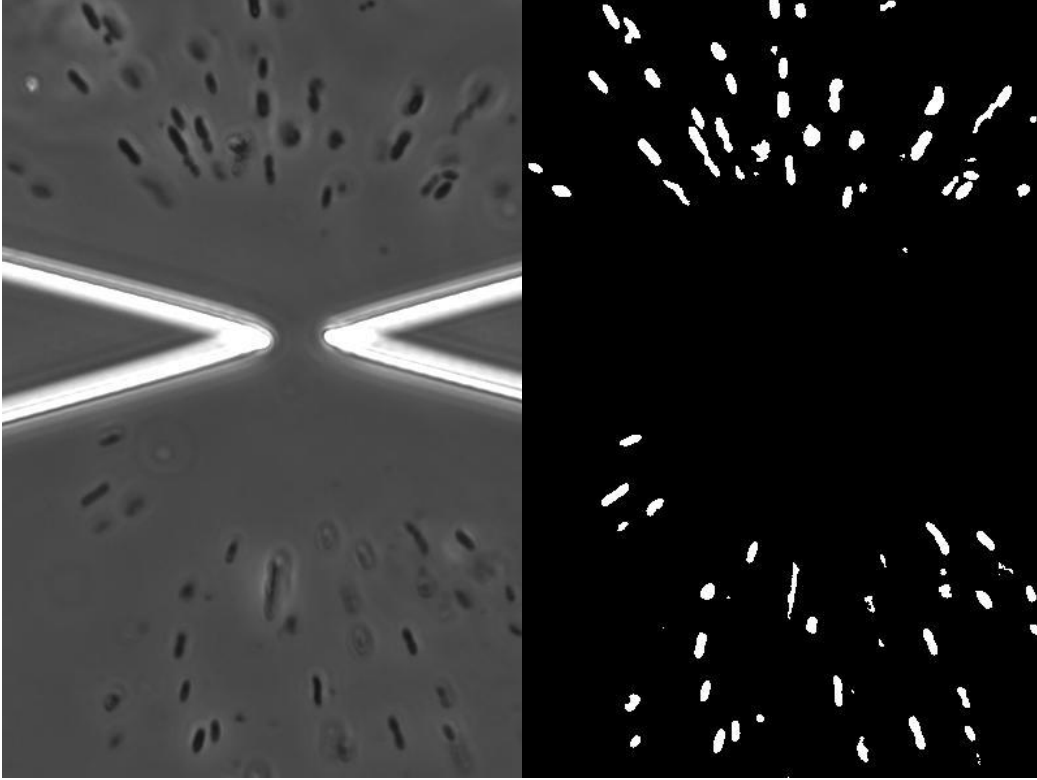
2.2 Pre-processing the Tracking Video

Figure 6a.The original image.   Figure 6b.The image after thresholding processing.

With camera and microscope, grayscale images could be recorded by the number of frames per second which is from 1 to 100.In this thesis, the images of ten frames per second are recorded for samples. The processing of particle from stationary to movement by DEP force is observed from beginning to end in the region close to the center point. To obtain the reasonable information, Thresholding method, the simplest method of image segmentation, is used to find the position of each particle effectively. Binary images are created after the thresholding from a grayscale image. If the image intensity $I\{i,j\}$ is less than some fixed constant T ($I\{i,j\}<T$), pixels in an image is replaced with a black pixel. If the image intensity is greater than that constant T ($I\{i,j\}>T$), pixels in an image is replaced with a white pixel.

After this processing, the position, radius, and shape of each particle could be indicated clearly. Some fragments with the smaller area that are caused by the bubbles or impurities in the medium are treated as noise and need to be removed. By setting a bound value of an area size, if the size of fragment area is less than the bound value, it will be deleted.

Since the electrical field distribution is symmetrical in z-dimension, the gradient of an electric field in z-dimension(i.e. normal to the chip) could be neglected, thereby allowing us to neglect displacements in this dimension The DEP force could be quantified by tracking particle displacements in x and y dimensions.

To locate the exact position of each particle, the centroid of the particle in two dimensions is defined as its position. The center of tips of two insulators is defined as a reference point. The coordinate (x,y) of it is (0,0) and this is used as the reference for setting positions of all particles. Pixel is used as a unit for recording in (x,y) coordinates. When the exact position of each particle is located in different frames, the identical particle must be matched with itself accurately in different frames. Thus, the displacement, velocity, and acceleration of each identical particle can be calculated by equation (1.16). Then the DEP force is quantified.
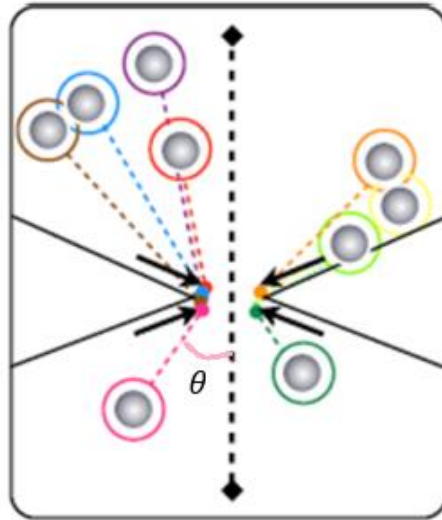
2.3 The Algorithm for Tracking

Figure 7. The angle of moving particle near reference region [13]

To match the position of each identical particle in different frame accurately, a matching algorithm needs to be developed. The movement of particles near the reference region is affected mainly by the direction of the DEP force. With equation (1.15), the direction of friction is opposite to the DEP force. It does not change the direction of particle

movement. Figure 6 shows that the trajectory of particles moving near the region of the reference point is near to a straight line. That is, the moving angle θ is almost unchanged when the particle moves in this region under the DEP field. The algorithm for matchings particle can be developed based on this characteristic.

The algorithm is introduced as follows:

1. If total frame number in tracking is M. Set the initial frame to be the 1st frame, the last frame to be M^{th} frame.

2. Select first two frames to determine the initial moving angle of the particle.

3. If particles are not highly concentrated at some region in 1st frame, for any particle in the frame, the nearest particle to it in the 2nd frame is assumed as the next position. Use these two positions to compute the initial moving angle θ_{12} and the moving displacement D_{12} of a particle. The moving angle θ_{12} represents the angle between moving direction of the identical particle from 1st frame to 2nd frame and the center line is shown in figure6.The moving displacement D_{12} represents the displacement of the identical particle from 1st frame to 2nd frame.

4. To decide the next position of an identical particle, find out the nearest three particles in 3rd frame for each particle in the 2nd frame. D_{23} and θ_{23} are the displacement and moving angle of them respectively.

5. Set D_{bound} and θ_{bound},which is usually $15°$, as the limiting factors to limit the searching scope for next particle. D_{bound} is a searching scope for the next position of the particle. It is adjustable and base on the movement of particles and is usually set to the value of 5 times of the average diameter of particles. For those three particles found in step 4, check each one of them whether the displacement $D_{23} < D_{bound}$ or not. For those particles whose displacement,$D_{23} < D_{bound}$, then check the moving angle $|\theta_{12} - \theta_{23}| \leq \theta_{bound}$ or not. In the end, choose the one whose $|\theta_{12} - \theta_{23}|$ is the minimum to be the next position of the identical particle.

6. Repeat step 5 for all the particles in following frames until reach M^{th} frame and the tracking is over.

7. For the identical particle in the nth frame in the tracking process, if there are no particles in $(n+1)^{th}$ frame satisfying the limitation in step 5, then use twice D_{bound} as the new D_{bound} and do the same work in $(n+2)^{th}$ frame. Then find out the next identical particle in $(n+2)^{th}$ frame. If the next position is found in $(n+2)^{th}$ frame, the particle position in $(n+1)$ frame is determined by the interpolation of the center position of two points. If a new particle cannot be found, the particle is considered missing and the tracking of this particle is over.
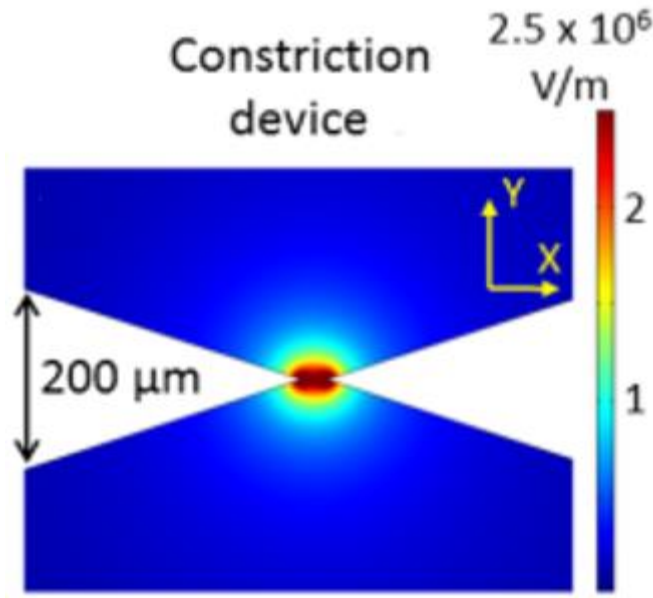
2.4 Normalized DEP Force in a Constriction Chip

Figure 8.The electric field in the device [13]

Figure 8. shows that the magnitude of electric filed is different in various position in the constriction device. By equation (1.7), with the same value of ε_m and the AC frequency, the larger the $\nabla|E^2|$ and the value of lr^2 are, the larger DEP force on the particle. DEP force is the main factor in the moving of particle, especially at displacement levels near to the reference point. For particle positions further away from the reference point, the influence of the DEP force decreases. To compare the DEP force on particles at different positions, the effects of the spatial non-uniformity of the electric field at different positions, as well as any variations in particle size must be counted for, thereby updating the results accordingly.

21

The product of electric field and its gradient can be calculated using the COMSOL Multiphysics software. A weighting function is extracted to account for the non-uniformity of electric field as following:

$$N(\nabla|E^2|, x, y) = \frac{MAX(\nabla|E^2|)}{\nabla|E(x,y)^2|} \tag{2.2}$$

. $MAX(\nabla|E^2|)$ is the maximum E∇E value in the device. The Normalized DEP force between position one(x1,y1) and position two(x2,y2) is the product of the measured DEP force between these two positions and the average of the weighting values where the positions are:

$$Normalized\ Fdep = Fdep \cdot \frac{(N(\nabla|E^2|,x1,y1)+N(\nabla|E^2|,x2,y2))}{2} \tag{2.3}$$

To Normalize the DEP force for different particle sizes, in ellipsoidal particles the size-weight function is defined as:

$$Normalized\ Fdep = Fdep \cdot \frac{l_{average} \cdot r_{average}^2}{l_{particle} \cdot r_{particle}^2} \tag{2.4}$$

$l_{average}$ and $r_{average}$ are the averages of lengths and radii of *Clostridium difficile* particles. $l_{particle}$ and $r_{particle}$ are the values of the length and the radius of the measured particle.

By combining equation (2.3) and (2.4), the normalized $Fdep$ after the normalization of a E∇E value and a particle size is:

$$Normalized\ Fdep = Fdep \cdot \frac{(N(\nabla|E^2|,x1,y1)+N(\nabla|E^2|,x2,y2))}{2} \cdot \frac{l_{average} \cdot r_{average}^2}{l_{particle} \cdot r_{particle}^2} \tag{2.5}$$

By equation (2.5), with the same value of ε_m and the AC frequency, the larger the $\nabla|E^2|$ and the value of a^3 are, the larger DEP force on the spherical particle. To compare the DEP force on different particles in different positions in the fair standard, the normalizations of $\nabla|E^2|$ and a^3 is necessary. The normalized function for the spheral particle is as follows :

$$Normalized\ Fdep = Fdep \cdot \frac{(N(E\nabla E,x1,y1)+N(E\nabla E,x2,y2))}{2} \cdot \frac{a_{average}^3}{a_{particle}^3} \tag{2.6}$$

$a_{average}$ and $a_{particle}$ are the values of the average radii of spheral particles and the radius of the measured spheral particle respectively.
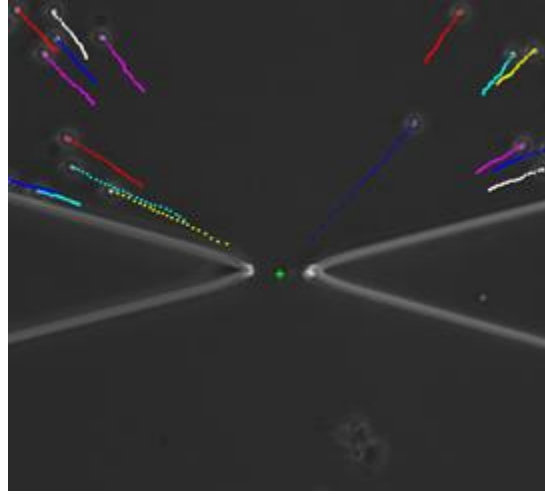
2.5 Velocity Analysis to Quantify DEP force

Figure 9. The trajectory of *Cryptosporidium parvum* particle.

In Figure 9, the routes of different cells are marked. By these symbols in a different color, tracking of different *Cryptosporidium parvum* cells by P-DEP force from the outside toward center are recorded.

The green star showed the reference point, which is the central position of two tips of triangle insulators. The closer the reference point, the stronger the gradient and magnitude of field is. Based on equation (1.5) and (1.7), the DEP force on the particle is proportional to the product of electric field and its gradient. Thus, the closer the reference point, the larger the DEP force, and the longer the moving displacement of the particle at the same time.

In Figure 7, the movement angle of a particle is related to the gradient of electric field. As shown in Figure 8, the field gradient decrease symmetrically from reference point to outside. So the change of the angle of the particle movement in the tracking process is small. Thus, the moving trajectory resembles a straight line.

The quantifying results of three particles are as follows respectively:

I.*Clostridium difficile:*

The relationship between the velocity and the distance from reference point for different *Clostridium difficile* particles are plotted as following:
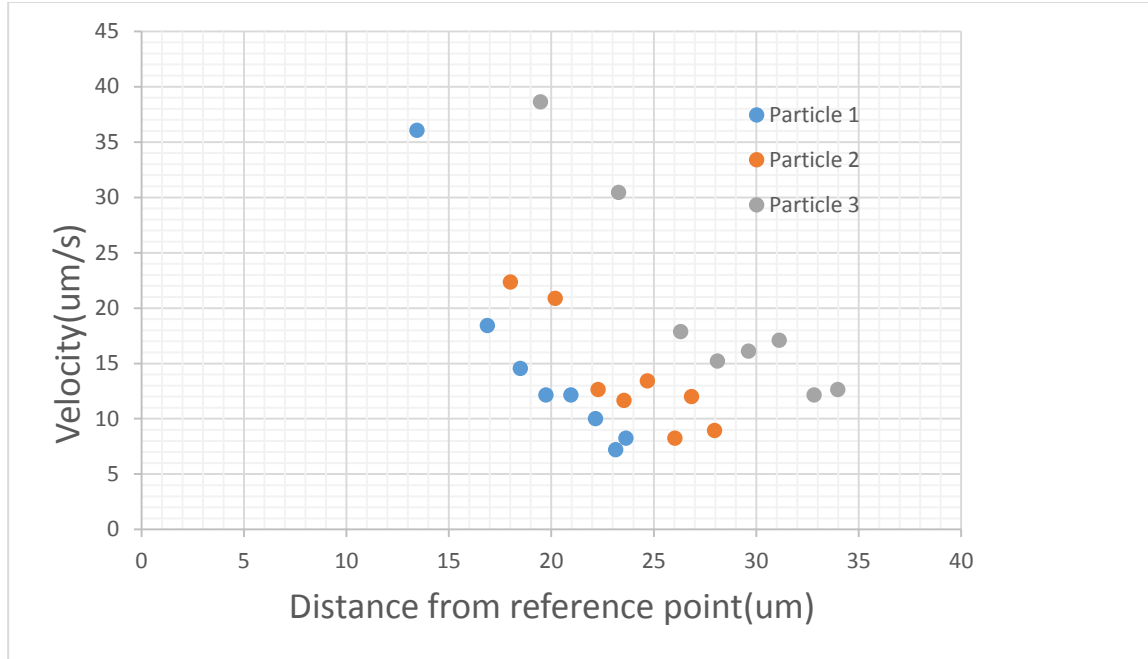
Figure 10. The velocity of *Clostridium difficile* particles in different position at 100 kHz AC electric field

Figure 10. shows that the velocity of different *Clostridium difficile* particles at 100 kHz AC electric field as a function of its distance to the reference point. The closer reference point, the higher n-DEP force on the particle and faster is its velocity. For most of *Clostridium difficile* particles, the velocity ranges from 5 to 40 µm/s at the distance of 10-40 µm from the reference point.

DEP force and velocity, both decrease with the increasing of distance from the reference point. The DEP force then is quantified by equation (1.12) and (1.15), the relationship between the force and the distance from the reference point for different *Clostridium difficile* particles are plotted as following.
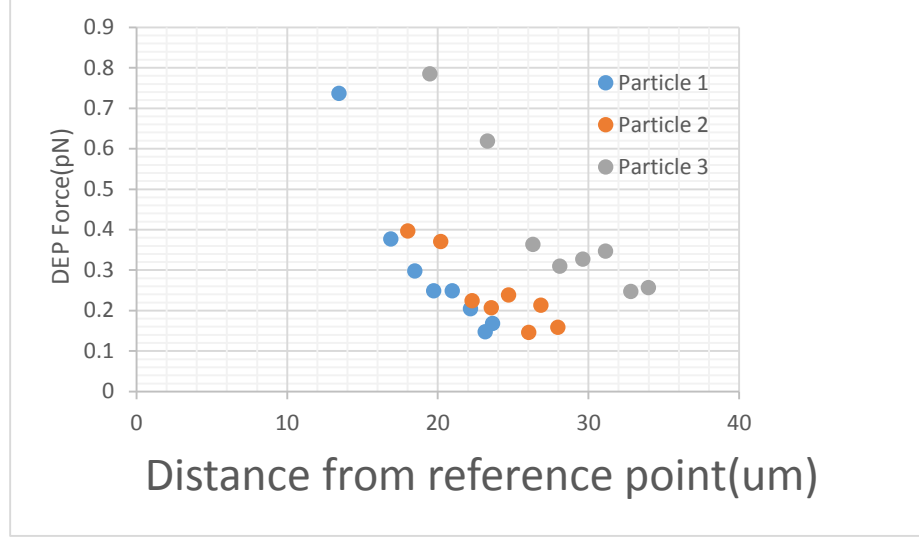
Figure 11. The DEP force of *Clostridium difficile* particles in different position at 100 kHz electric field

Comparing Figures 10 and 11, the trend is similar. Due to the mass (10^{-12} g) of *Clostridium difficile* particle is very tiny. By equation (1.15), the DEP force can be calculated almost by $F_{DEP} = fv$. For an individual particle, the value of DEP force exerts on it approximates to its velocity multiplied by a friction factor f. The DEP force on the individual *Clostridium difficile particle* ranges from 0.1 to 0.8pN.

After the normalizations of size and $\nabla|E^2|$ by equation (2.5), the *normalized* DEP force could be compared fairly. The results after the normalizations are plotted as following.
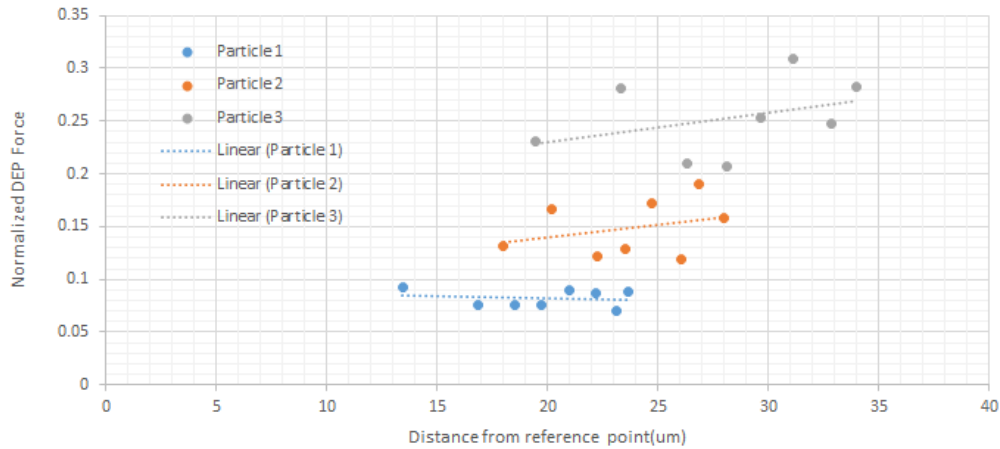

Figure 12. The Normalized DEP force of *Clostridium difficile* particles in a different position at 100 kHz electric field.

As showed in figure 12, the particle is forced on the same normalized DEP force and presented a horizontal straight line with the distance. Though the resolution of the image may cause a calculation error and a dispersion of data, the result satisfies Equation (1.9).In previous research, n-DEP force is very hard to measure due to the reference position of moving particles is not easy to define. The initial position of a particle caused by n-DEP is usually not close to the reference point. The result indicates that after normalization, the initial position of a particle is no longer the problem due to the effect of $\nabla|E^2|$ in various position is eliminated.

Equation (1.22) indicates that the magnitude of the CM factor of different ellipsoid particles is different apparently because of their major axes and minor axes are different. The polarizability of each *Clostridium difficile* particle are various due to their size are not the same. It causes the trend of their *normalized* DEP force different.

	Before normalization	After normalization
particle1	3.5×10^{-2}	7.5×10^{-5}
particle2	8.4×10^{-3}	7.1×10^{-4}
particle3	3.6×10^{-2}	1.3×10^{-3}

Table.1 Variance of DEP force exerted on *Clostridium difficile* before and after normalization

Table.1 shows the DEP force variance of each *Clostridium difficile* before and after normalization. After normalization, the variance of these force are reduced to less than one-tenth. It means that the differences between forces in various positions are reduced greatly by normalization.

II. *Cryptosporidium parvum*

The relationship between the velocity and the distance from reference point for different *Cryptosporidium parvum* particles are plotted as following:
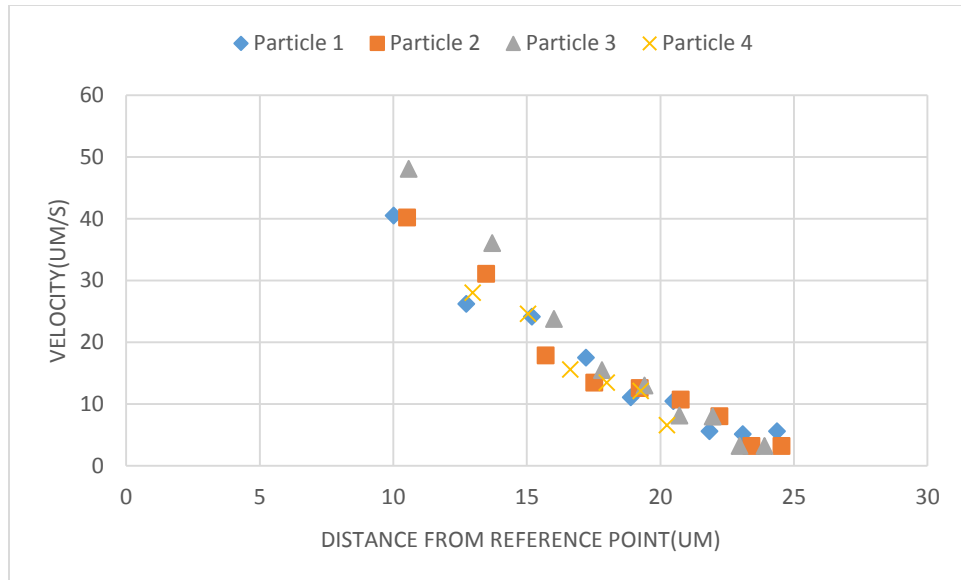
Figure 13. The velocity of *Cryptosporidium parvum* particles with heat treatment in different position at 400 kHz electric field

From the figure 13, the closer the reference point, the larger DEP force on particle and the faster the velocity of a particle. Particle 1 and 2 have the larger change of velocity and others have smaller relatively. The velocity of particles ranges from 2 to 50um/s.

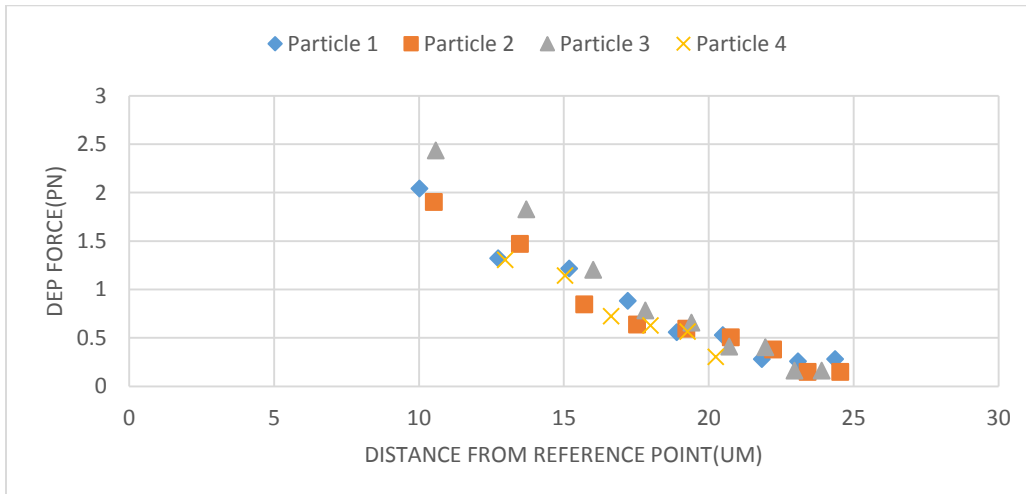The DEP force exerted on particles are quantified and presented the following figure.

Figure 14. The DEP force of *Cryptosporidium parvum* particles with Heat treatment in different position at 400 kHz electric field

The quantified values of DEP force of particles range from 0.1 to 2.5 pN. Because the mass(10^{-10}g) of *Cryptosporidium parvum* particles is very tiny, the force is calculated as velocity multiplied by friction constant, the trend of particles is similar to Figure 13. The DEP force on particles decrease with the increasing in distance from the reference point.

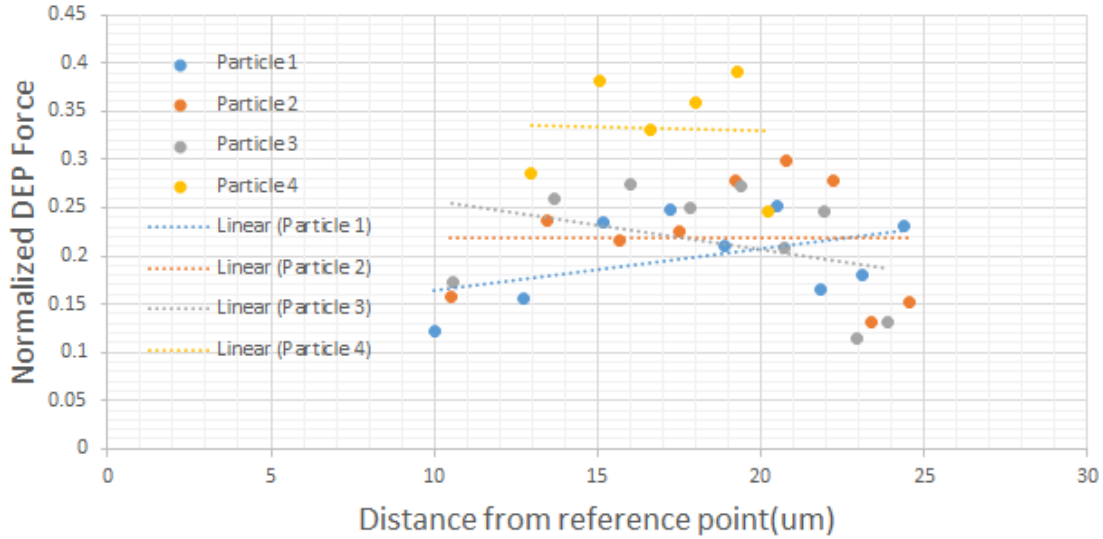These DEP forces are normalized and presented as following figure.

Figure 15. The Normalized DEP force of *Cryptosporidium parvum* particles with Heat treatment in a different position at 400 kHz electric field

Figure 15 shows the effect of the normalization clearly. Though the image resolution causes an error in computation, the distribution of forces on the range are almost horizontal lines. The trend of the straight line is near flat and the result of normalized DEP force of each *Cryptosporidium parvum* satisfies Equation (1.9).

Equation (1.21) indicates that the magnitude of the CM factor of different spheral particles are different slightly if their size is not much different. The polarizability of each *Cryptosporidium parvum* particle are similar due to their size are not much different. It causes the dispersion of their normalized DEP force trends are close to each other. However, the dispersion of particle 3 is obviously different from other particles. The reason is that the wounded degree of particle 3 by heating is different from other particles and this causes the polarizability of it changes.

	Before normalization	After normalization
Particle 1	0.37	2.1×10^{-3}
Particle 2	0.35	3.7×10^{-3}
Particle 3	0.62	3.8×10^{-3}
Particle 4	0.18	3.5×10^{-3}

Table 2. Variance of DEP force exerted on *Cryptosporidium parvum* before and after

normalization

Table.2 shows the DEP force variance of each *Cryptosporidium parvum* before and after normalization. After normalization, the variance of these force are reduced to less than one percent. It means that the differences between the magnitudes of forces in various positions are reduced greatly by normalization.

III.HEK cell

The HEK cell is the largest cell among three subjects. The constriction gap is near 10um to *Clostridium difficile* and *Cryptosporidium parvum*, respectively but 30 um to HEK cell. The velocities of HEK cells in different positions is shown in Figure 15.
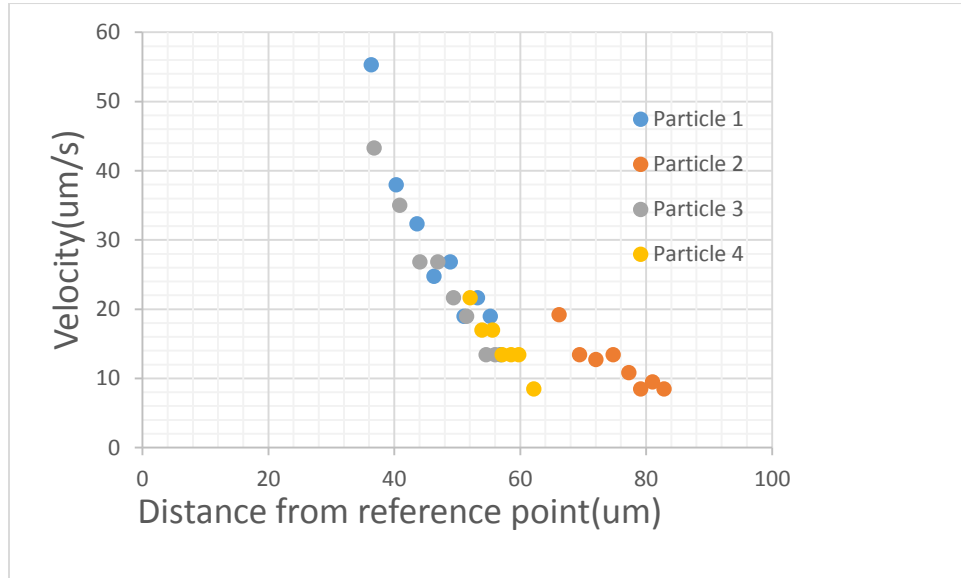

Figure 16. The velocity of HEK cell in different position at 500 kHz electric field

The closer the particle to the reference positions, the larger the DEP force on the particle. Figure 16 shows that the highest velocity is at the distance of 35 um from the reference point. The further the distance from tips, the weaker the DEP force on the particle and the slower the movement of a particle.

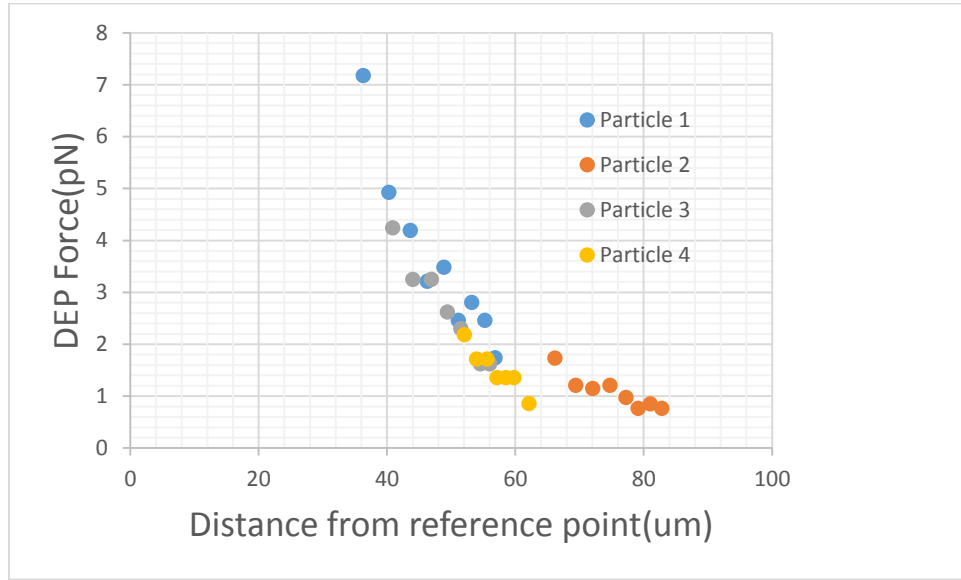The quantified DEP force is shown in Figure 17:

Figure 17. The DEP force of HEK cell in different position at 500 kHz electric field

In spite of the largest size of three subjects, the result of figure 16 and figure 17 showed that their data distribution is very similar because the mass (2.5ng) of HEK cell is still so small that the term of ma^2 can be neglected. The same as previous two samples, its DEP force could be recognized as the product of velocity and friction force. Figures 16 and 17 have the same trends of data distribution. The closer the particle near to reference point, the stronger DEP force on the particle. The DEP force for the most particles ranges from 1-8pN. The DEP force and polarization degree are related to the number of dipoles. By equation (1.6), the DEP force is related to the radius of the particle. For the micrometer size of cell, the larger the volume, the more the dipole number in polarization. So the HEK cell has the larger DEP force among three bioparticles. These DEP forces are normalized by equation (2.6) and presented as following figure.
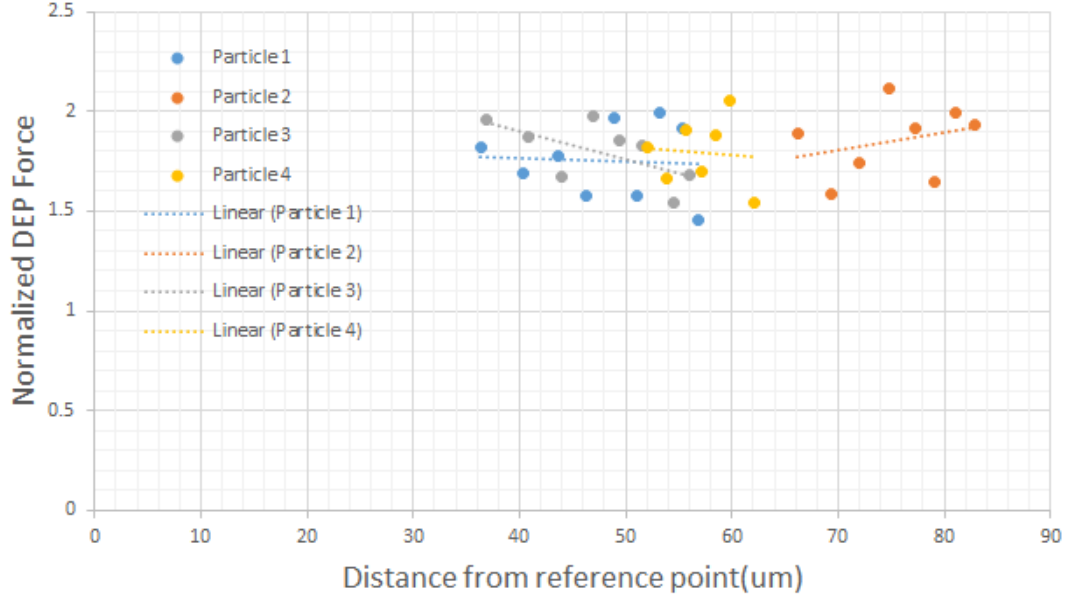
Figure 18. The Normalized DEP force of *HEK cells* in different position at 500 kHz electric

After normalization, the DEP force on each HEK particle can be compared on the same basis. By Figure 18, the distribution of normalized DEP forces shows a horizontal direction. The result satisfies Equation (1.9). By Equation (1.21) ,the magnitude of the CM factor of HEK cells are almost the same because of their size are not much different. Thus, the polarizability of each HEK cells is similar. It causes the dispersion of their normalized DEP force trends are in the close range. Moreover, though the route of particle 2 is different from other particles, it is attracted to the tip along the side of an insulator. The normalized result of it is still similar to other particles.

However, the dispersion in the distributions is caused by the image resolution on the measured displacement and the larger volume of the particle. Since the pixel represents the unit of distance, the change is acute even for a difference one of a single pixel. The position of a cell is determined by its centroid. The radius of an HEK cell is near to 10 pixels. The $E\nabla E$ value of each pixel in an HEK cell area is different. When the change of $\nabla|E^2|$ is so drastically in space and the normalization to eliminate the effect of $E\nabla E$ is only performed on the position of the centroid, the DEP force on the particle is over-estimated. At particle positions closer to the constriction tip, the over-estimation is more serious.

	Before normalization	After normalization
Particle 1	2.72	0.052
Particle 2	0.20	0.023
Particle 3	1.61	0.036
Particle 4	0.38	0.043

Table 3. Variance of DEP force exerted on HEK cell before and after normalization

Table.3 shows the DEP force variance of each HEK cell before and after normalization. After normalization, the variance of these force are reduced to less than one-eighth. It means that the differences between forces in various position are reduced greatly by normalization.
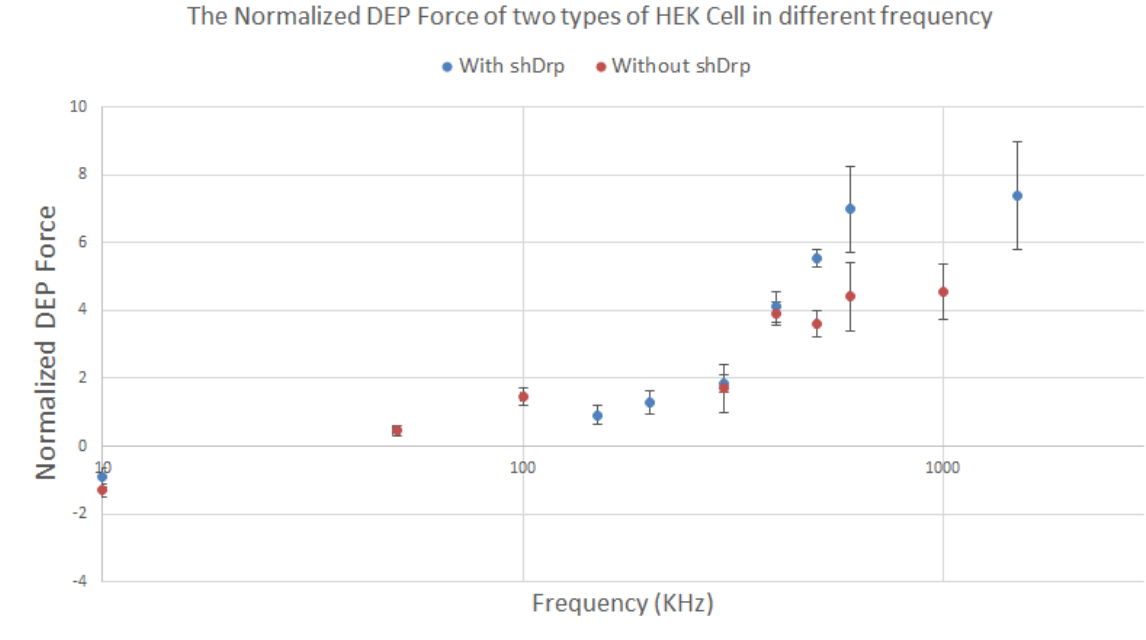
2.5 DEP Force Spectrum of HEK Cell

The Normalized DEP Force of two types of HEK Cell in different frequency
● With shDrp   ● Without shDrp

Figure 19. The Normalized DEP force spectrums of two types *HEK cells* in 300uScm ε_m

The normalized DEP force spectra were plotted by the average normalized DEP force of particles at different frequency values. Figure 19 shows that the normalized DEP force spectrums of two different types of HEK cells with error bars. These spectrums could be considered the real part of Clausius-Mossotti factor with frequency and describe the dielectrophoretic characteristics of particles. The crossover frequency of HEK cell with shDrp is about 40Khz and it is about 70Khz without shDrp. More importantly, this method allows us to conclude that the pDEP force levels on Ras-modified Hek cells with a highly

fragmented mitochondrial structure is significantly lower than that obtained on the same cells after shDrp modification to cause a highly connected mitochondrial structure.
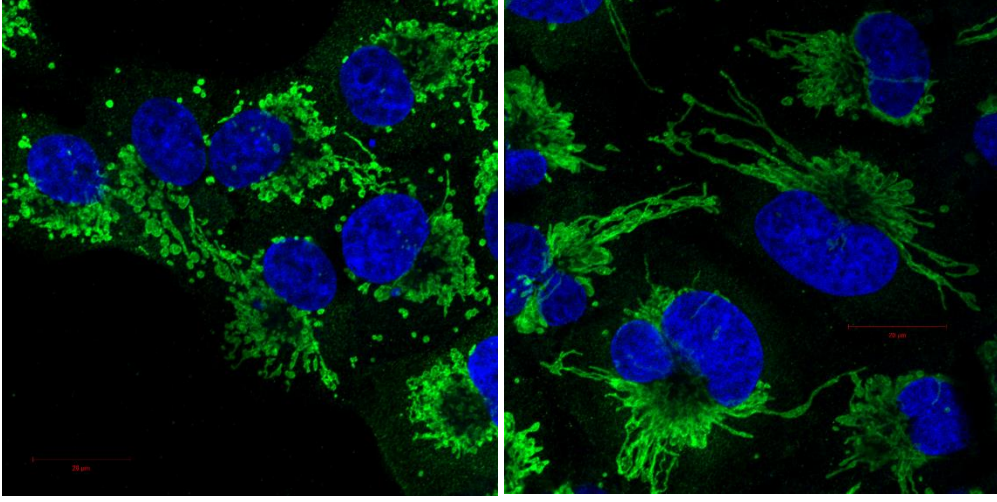

Figure 20a. HEK cells with shDrp.   Figure 20b. HEK cells without shDrp

	Without shDrp	With shDrp
Diameter	20um	20um
Membrane Thickness	13.5nm	15nm
$\varepsilon_{membrane}$	5	3.5
$\sigma_{membrane}$(s/m)	1.5×10^{-5}	1.5×10^{-5}
$\varepsilon_{cytoplasm}$	60	60
$\sigma_{cytoplasm}$(s/m)	0.15	0.6

Table 4. The dielectric properties of two types of HEK cells

Table 4. shows the result of the dielectric properties of different types of HEK cells by using a non-linear least squares fitting the routine from equation (1.21). The most difference between them is the value of their $\sigma_{cytoplasm}$. The cytoplasm conductivity of HEK cells with shDrp is four times larger than that without shDrp. This indicates the mitochondrial structure in the cytoplasm is different in this two types of HEK cells. Figure 20a and 20b show the different mitochondrial structure which is the green areas.

From the above results, the equation (1.9) satisfies the results from these three different particles. Thus, the image processing method that developed in this study for normalized DEP force of three types of bioparticles is reasonable and useful.

Chapter 3
Spatio-Temporal Analysis Measurements

By the equation (1.19) and (1.21), we can quantify the direction and magnitude of the relative DEP force by analyzing the change of cell concentrations. The relative DEP force spectrum can be plotted to describe the dielectrophoretic characteristics of particles, discriminate cell species and evaluate the changing degree of cells after different treatments.

3.1 DEP Well
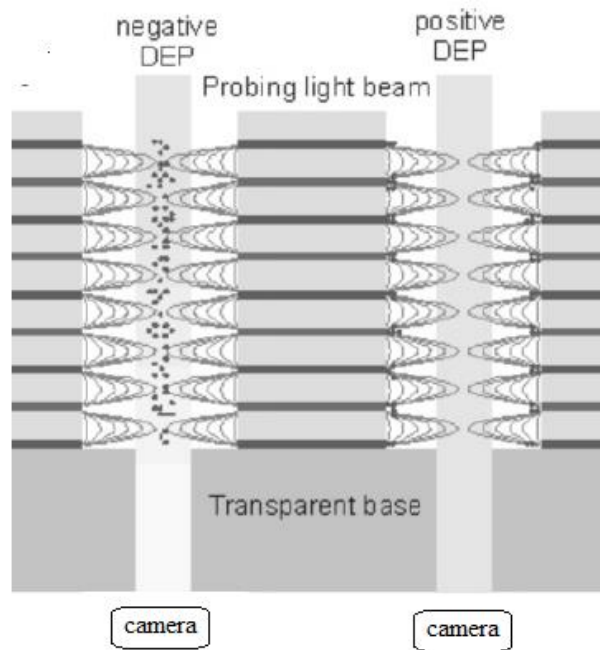
Figure.21 A structure of DEP Well[23]

Figure 21. shows that a DEP-Well systems are made by a laminate of alternating insulating layers and conducting material. A signal generator connected to these conducting layers ensures all electrodes are in the same polarity. The "rolled-up" two-dimensional electrode array is manufactured by drilling channels through the laminate. The resulting wells with alternate potential electrodes separated by insulating layers.

The measurement of the DEP effect for this DEP-Well system is an absorption measurement technique [23]. When the electrodes are energized, P-DEP pulls particles from the center of the side of the well and N-DEP repelled them into the center of the well. The magnitude and direction of the particles can be detected rapidly. By using a light source to illuminate the well, the change of fluorescence intensity could be observed from the opposite side of the well. The change is due to the redistribution of particles and could be used to quantify DEP force.

To improve the limitations of time consuming, laborious and limited number of sample, a novel device, a 3DEP reader was developed as a chip with 20 wells. The device includes 3D well structure like a microtiter well plate, electrodes along the inner surface. The special design of this system is to use the composite laminate conductor to produce electrodes with similar dimensions. The structure is around the walls of a hollow cylinder. Because of many parallel electrodes can be operated simultaneously, samples are tested separately in the predetermined conditions. Large numbers of experiments can be performed at the same time.
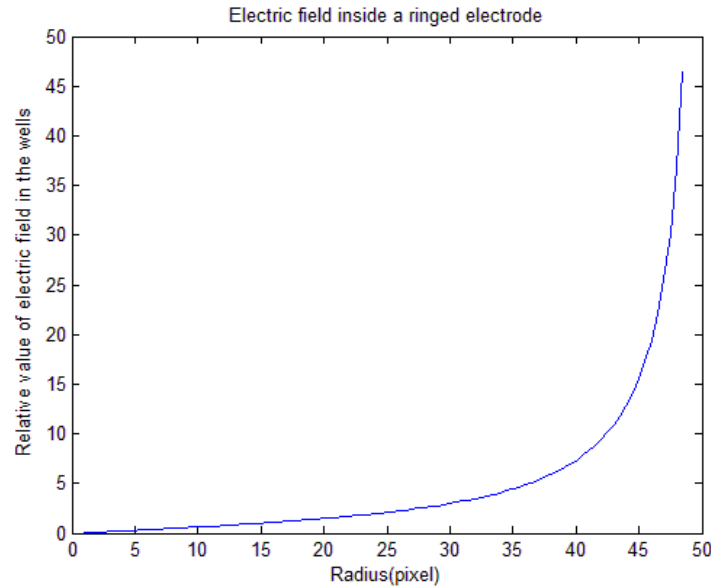

Figure 22. The electric field intensity attenuates from a side of ringed electrode to a center of a well [24]

Since electrical field distribution inside a well is symmetrical, the electrical field intensity is related to the radius and it can be expressed as figure 22. Field intensity

attenuates from a side of a ringed electrode to a center of well and it is zero at the center (Figure 22). From the equation (1.6), DEP force is related to the gradient of the square of the electrical field intensity. So it is stronger near a side of a well and equal to zero at center. The P-DEP attracts the cells suspending in medium to the ringed electrodes, so cells accumulate at the edge of the well. In contrast, N-DEP pushes the cells away from the electrodes to the center, hence, the cell concentrations and consequently the light intensity is decreased in the region near the electrodes, but increased in the region near the center.
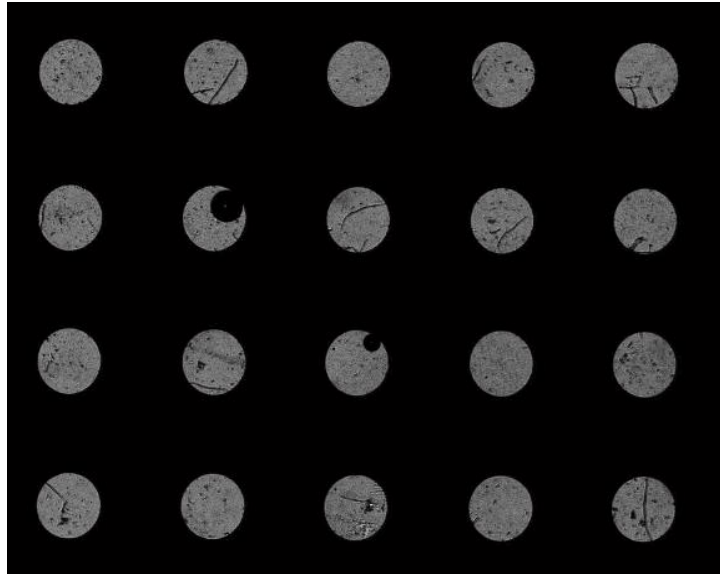
3.2 Pre-processing the Video

Figure 23. Clostridium difficile samples in the wells with 20 different frequencies

The chip "3DEP reader" that contains 20 microfluidic wells with ringed electrodes can measure the particle displacements under dielectrophoresis in each well, at 20 different frequencies, applied simultaneously at each well (the signals from particle scattering due to DEP motion are shown in Figure 23). In this study, based on spatio-temporal analysis of light scattering due to particle translation. A new methodology which can offer a detailed information for the behavior of particle population under DEP force and implement rapid quantification of DEP spectra is developed.

In the processing of cells analysis, the same kind of cell samples was placed into 20 wells. The ringed electrodes provide the different electric field with different frequencies ranging from 50KHz to 45MHz. A grayscale image of cell samples was taken per second

and the total record time was 30 sec. Figure 24 shows that the radius of each well was 50 pixels in the images and the well region was divided into 9 ringed parts with a width of 5 pixels .The first ring region is the area between the radius of 3 pixels and 8, and the least ringed region is the area between the radius of 43 pixels and 48. The average pixel intensity of ringed region between different radii in the well was calculated to analyze the change rate in the different region of the well. The difference of average intensity between the frame and its previous frame in the same region was served as the change of intensity in that region. By this method, the changing rate of cells concentrations at a different time and in different regions could be found with these 30 figures. The change rate of intensity then is further analyzed to quantify the DEP force.
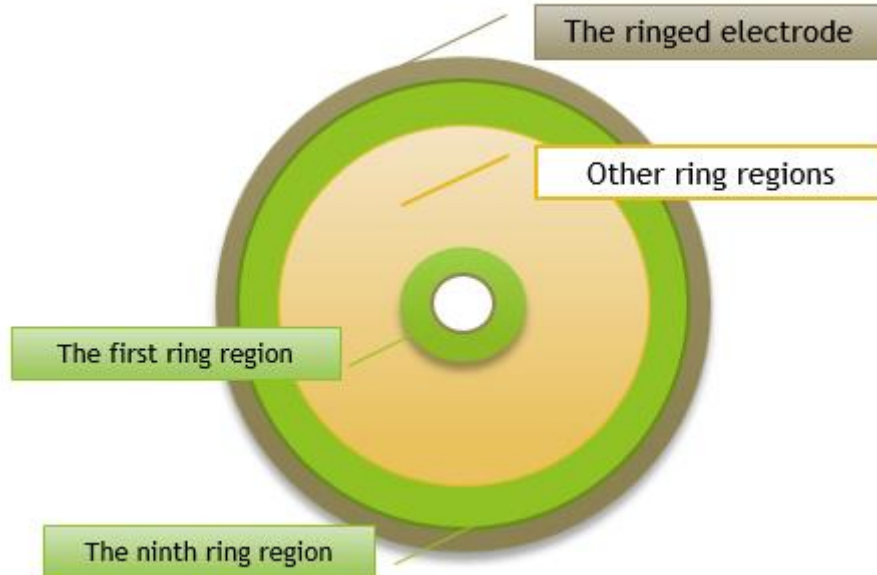

Figure 24. The ringed electrode of the well and different ring regions in the well

Figure 25. The effect of bubbles of the original figure and after thresholding.

In some samples, calculation of the intensity was interrupted by the bubbles adhered to the wall of the well or some impurities in the medium. As left figure shows, the black points in the sample region were impurities and the larger black circle area was a bubble. They did not be moved or changed by the effect of DEP force. The pixel image of this regions were all black in the record processing. They could be removed by thresholding method. As right figure shows, after setting the bound of the intensity value, the positions of pixels that its intensity was lower than the bound value were black, and they are excluded in the processing of the calculation of the average intensity. The positions of pixels that its intensity was higher than the bound value were white, and the intensity of these pixels must be calculated for the average intensity in the region. By this process, the interrupt of noise could be eliminated effectively.

After eliminating the effect of these noise parts, the changing rate of concentrations in 9 different ringed regions was computed with frames as follows.

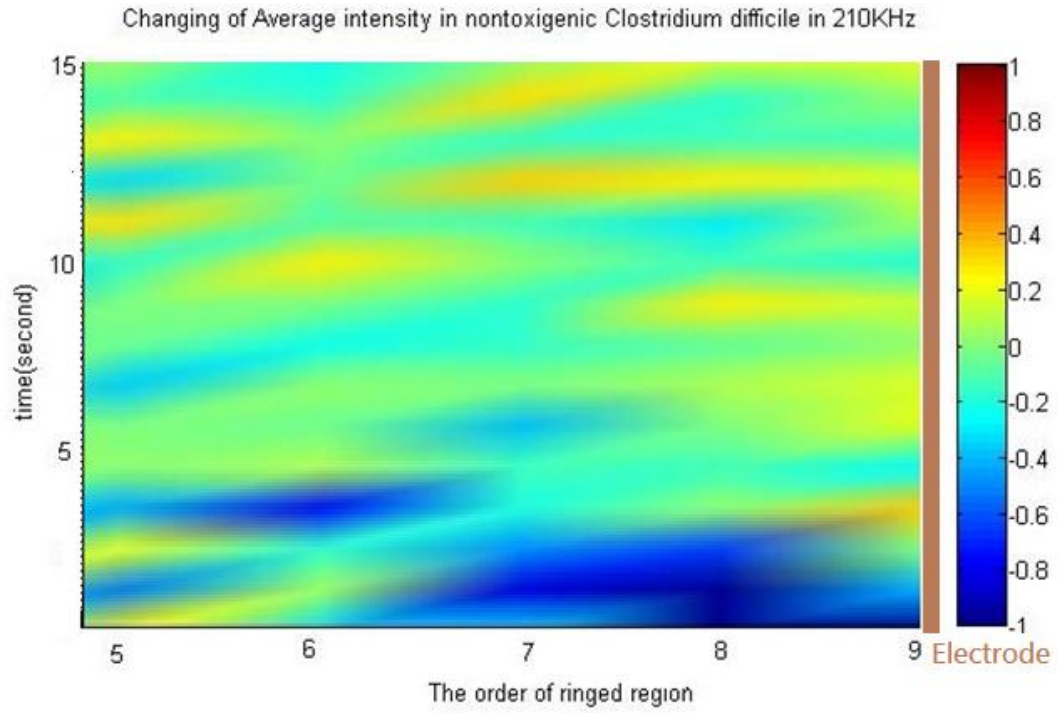## 3.3 Spatio-Temporal Analysis of Cell Population Concentrations

Figure.26 The changing rate of concentrations at different regions and times in N-DEP case
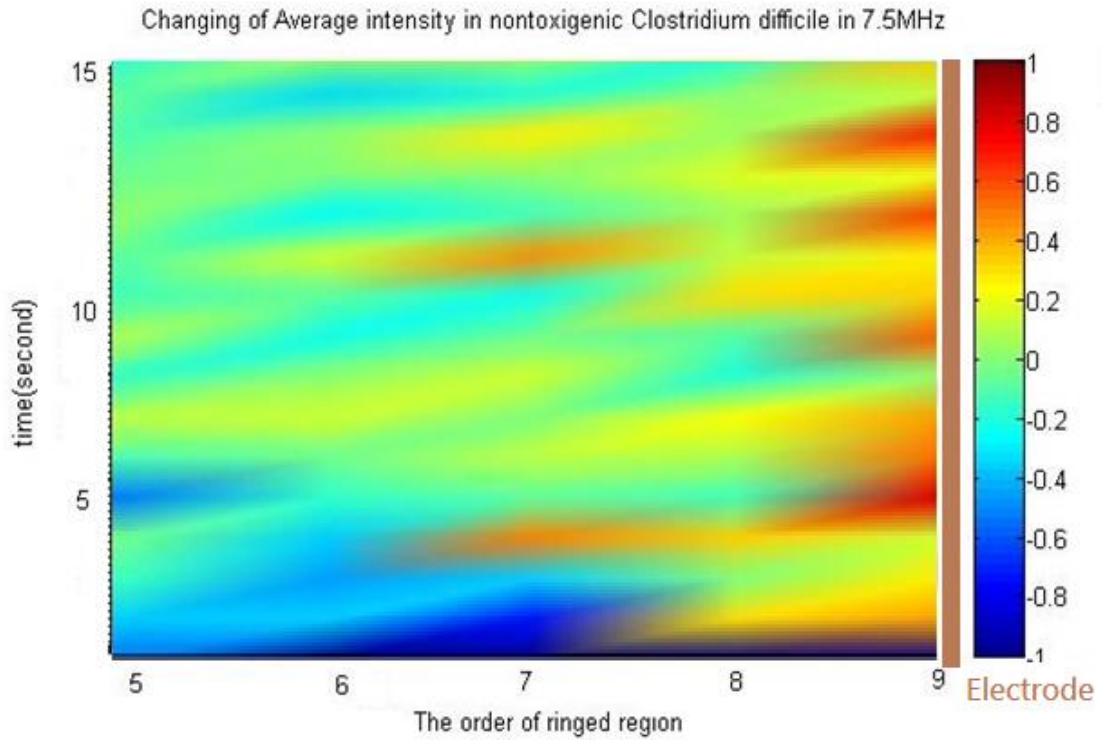

Figure.27 The changing rate of concentrations at different regions and times in p-DEP

Figure 26 and 27 presented the changing of concentrations at *Clostridium difficile* at different regions and times in two cases of N-DEP and P-DEP. The changing rate of concentrations in the region far away from the electrodes is effected by a noise like diffusion greatly. The figures only show the result from the fifth ring area to the ninth ring area because of DEP force only dominate in the region closer to the ringed electrodes. X axis represented the order of ringed regions in a well. Y axis is the time, a sample is recorded with 1 frame per second for the period of 15 seconds. The color bar indicates the changing rate of the average intensity. Figure 26 is the analysis of the lower frequency (210 KHz) and the figure 26 is of the higher frequency (7.5MHz).

In figure 26, the color shows that the change rate of concentrations is negative in most of the time at the regions which are closer to the electrodes. Especially in the time of 1 and 2 second, the color indicates a large amount of particle leave the region. After averaging the change rate of concentrations in the regions, the value of it is negative. That is, the concentrations near ringed electrode are decreased .The movements of particles are from edge to center. That is the function of N-DEP. Particles are pulled to center by the N-DEP force.

In Figure 27, the change rate of concentrations is positive in the region closer to the electrodes in most of the time. Therefore, the concentrations near the ringed electrode are increased .The movements of particles are from center to edge. That is the function of P-DEP. Particles are adsorbed to ring edges by the force.

3.4 Normalized DEP Force

By these figures, the effect of DEP forces on particles by different frequencies could be observed. The DEP force on particles at different regions can also be quantified. However, by equation (1.5), the DEP force is affected by electrical field intensity and gradients of intensity (E∇E). If we want to evaluate accurately the DEP force on particles in different frequencies, the effect of electrical field intensity and gradients of it need to be eliminated. To eliminate the effect of DEP force at different positions on the value of electrical field intensity multiplied by its gradients, the method by multiply a weight function:

$$N(\nabla|E^2|, r) = \frac{1}{\nabla|E^2|(r)}$$ (3.1)
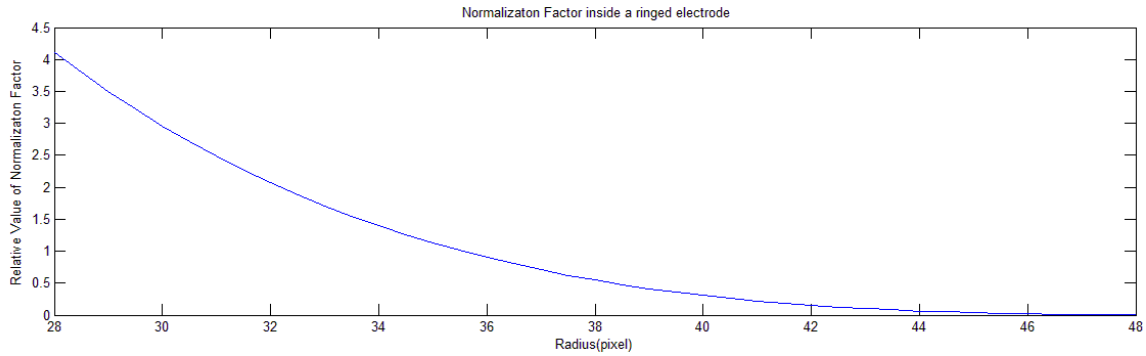
is called Normalization factor.

Figure 28. The value of the normalization factor in different radius of well

Figure 28 shows the value of weighting function with different radius of a well. The intensity of each pixel for all samples is multiplied by the normalization factor of its radius. After the normalization, the relative normalized DEP force in different radius can be compared on the same basis.

The strongest DEP force is at the edge of the well. DEP force decreases along the radius toward the center of a well with decreasing of position's radius and the force is zero at the center. In other words, when the radial position increases, DEP force becomes the dominate force for the net force. For the regions of smaller radius, the dominant effect of DEP force become small and the effect of noise enlarges. The change of concentration intensity is amplified hundred or thousand times by the normalization. Some background noises and diffusion force on the particles are also enlarged. So the results from the smaller radius are not reliable. In this study, only larger radii are considered as reliable samples to quantify the DEP force because it is dominant there.

3.5 DEP Force Spectrum of *Clostridium difficile*

The average changing rate is calculated from a ring area between the radii which are 43 and 48 pixels is served as a relative DEP force. The region to quantify the average DEP force is shown in Figure 29. The average DEP force represents the average changing rate of concentration in that area in 30 sec. Figure 30 shows two the relative DEP spectrums of different strains, the nontoxigenic strain and the hightoxigenic strain, of *Clostridium difficile* particles obtained through this analysis.
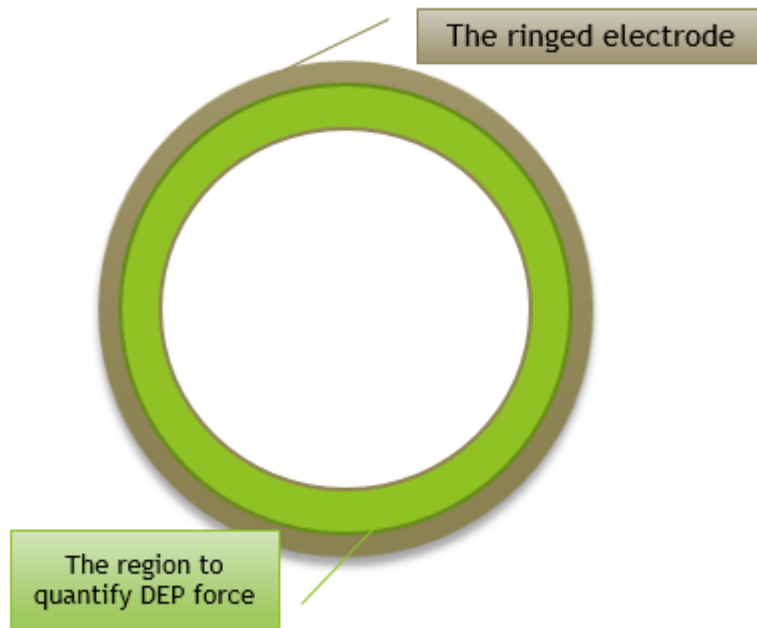
Figure 29. The diagram of the region to qualify average DEP force
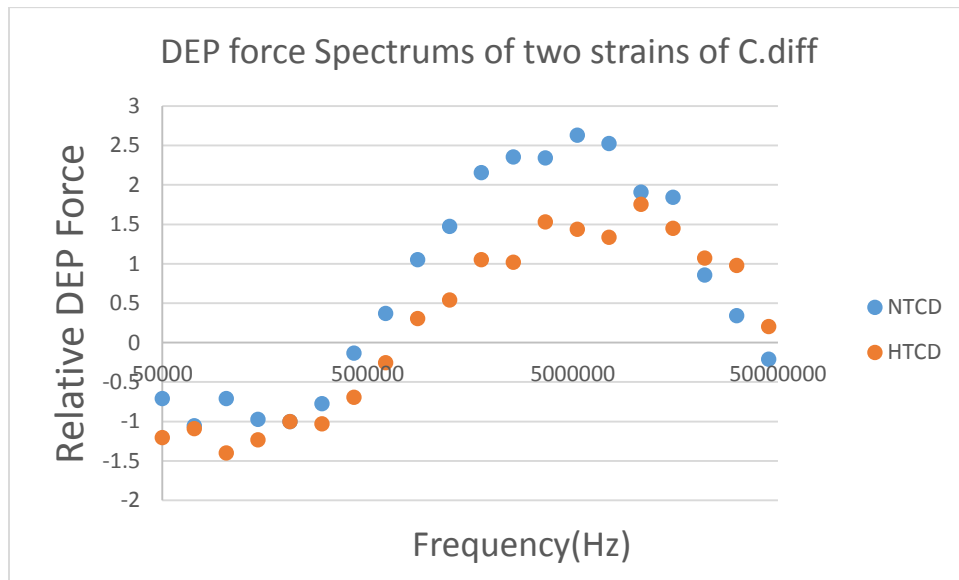
Figure 30. The relative DEP spectrum of two strains of *Clostridium difficile* particles

DEP spectrum can be used to express the P-DEP, N-DEP and the relative force of particle population in different frequencies. Figure 30. presents the relative DEP spectrum of Nontoxigenic *Clostridium difficile* particles. If the related DEP force > 0, particles are affected by the P-DEP force to a side of well. If the related DEP force < 0, particles are

pushed to the center of the well by the N-DEP force. The crossover frequency of this particle is 450KHz .When the frequency is less than 450 KHz, the particle is on the n-DEP force. In contrast, when the frequency is larger than 450 KHz, the particle is on the pDEP force. The critical frequency of Hightoxigenic *Clostridium difficile* particle is 700 KHz. When the frequency is less than 700 KHz, the particle is on the N-DEP force. In contrast, when the frequency is larger than 700 KHz, the particle is on the p-DEP force. More importantly, this method allows us to conclude that the pDEP force levels on Nontoxigenic *Clostridium difficile* is significantly higher than that obtained on the Hightoxigenic *Clostridium difficile.*

	HTCD	NTCD
Major Axis(um)	3.6	3.6
Minor Axis(um)	0.57	0.47
Wall Thickness(nm)	27	34
ε_{wall}	48	15
σ_{wall}	3×10^{-5}	5×10^{-6}
$\varepsilon_{cytoplasm}$	65	65
$\sigma_{cytoplasm}$(s/m)	0.48	0.65

Table 5. The dielectric properties of two strains of *Clostridium difficile*

Table. 5 shows the result of the dielectric properties of different strains of *Clostridium difficile*. The wall thickness of this two strains of *Clostridium difficile* is 27nm and 34(nm) [25].By using a non-linear least squares fitting the routine from equation (1.22). The most difference of them is the value of their ε_{wall}. The wall permittivity of High-toxic *Clostridium difficile* is three times larger than that of Non-toxic *Clostridium difficile*.

By this methodology, the relative DEP spectrum of different *Clostridium difficile* particles could be plotted and the dielectric properties of them could be calculated. The methodology can offer a detailed information for the changing rate of particle population in different regions and time. It is very useful and convenient to analyze the spatio-temporal changing of particle population because of its rapid quantification of DEP spectra.

Chapter4

Conclusion and Future Work

4.1 Conclusion

One of the advantages of the Dielectrophoresis (DEP) is the ability to enable the frequency-selective translation of particles under spatially non-uniform fields based on their distinctive impedance characteristics, so it is an effective technique for cell sorting and quantification. These techniques are utilized to analyze and characterize three kinds of bioparticles, *Cryptosporidium parvum*, *Clostridium difficile* and Human Embryonic Kidney (HEK) cell to validate a model for particles of different sizes and shapes.

By positive DEP (P-DEP) or negative DEP (N-DEP), particle translation towards or away from localized regions of high field occurs. Because of the bioparticle characteristics, the value and direction of their DEP force are varied at various electric frequencies. This work in this study is focused on using image analysis methods to quantify the translation of particles under spatially non-uniform fields to determine the DEP force spectrum versus frequency. Two different device designs were used.

The first is based on a constricted microfluidic channel, wherein image tracking is used to directly identify particle translation where the DEP frequency spectra is quantified with single-particle sensitivity. The second device uses a set of microfluidic DEP-Wells with ring electrodes. It can quantify quickly the DEP spectra based on spatio-temporal analysis of light scattering due to particle translation.

For the first method, the thresholding method is used to find the position, area and shape of each particle effectively. To obtain the reasonable information, some fragments with the smaller area which are the bubbles or impurities in suspensions are deleted by setting a bound value of an area. The DEP force could be quantified by calculating the tracking of particles in X-Y dimensions. An adequate algorithm is developed to match the position of each particle in its frame accurately. The relationship between the velocity and the distance from the reference point for the smallest samples of different three particles is presented.

By normalization, the effect of $\nabla|E^2|$ in a different distance on the DEP force on particles and the effect of size in different particles can be eliminated. Normalization can be used to present the polarization degree of an individual particle. For the particle that normalization is effective, its normalized DEP force did not vary with the distance from the reference point. That is, if the particle is close enough to the reference point, the calculated DEP force is reliable and no matter what the position is. However, if particles of larger size are too close to the regions of drastic change fields, it leads to over-estimation of the DEP force because of the uneven force across the whole particle. Despite this, the method that developed in this study for quantifying dielectrophoresis force of three kinds of bioparticles is reasonable and useful from the results of this study.

For the second method, the calculation of the intensity was interrupted by the bubbles adhered to the wall of the well and impurities of samples. Their effect could be removed by using thresholding method to recognize their position. The positions of pixels that its intensity was lower than predetermining bound value were excluded in the processing of the calculation of the average intensity and the interrupt of noise could be eliminated effectively. The methodology can offer a detailed information for the changing rate of particle population in different regions and time. The accurate relative DEP force on particle populations in different frequencies is obtained by eliminating the effect of electrical field intensity and gradients. Only the ringed region of larger radius are considered as reliable samples to quantify normalized DEP force because the DEP force is dominant there. This result indicated that the measurement performance of the DEP spectrum of particle populations can be quantified effectively and rapidly.

From the results of this study, these image tracking methods and the normalization method could serve as useful tools to quantify particle motion under force fields in microfluidic systems. It is useful for studying cellular subpopulations, which is of fundamental importance in biomedical sciences.

4.2 Future Work

The extension of our research is possible for future work. For the ellipsoid particle, the shape causes much difference in their polarizability. A future investigation of normalizing the polarizability is possible. Another extension of the first methodology may be with the algorithm in tracking. The correction rate and tracking efficiency are possible to be enhanced. Another possible study is to apply the two methodologies to other kinds of geometric devices. Then develops the normalization in the similar way to measure DEP force more accurate.

Bibliography

[1] Q. Cheng, H. Huang , L. Chen, X. Li, Z. Ge, T. Chen, Z. Yang and L. Su, "Dielectrophoresis for bioparticle manipulation" , *International J. of Molecular Sciences*, vol. 15, pp. 18281-18309, 2014.

[2] V. Farmehini, A. Rohani, Y. Su, N. S. Swami, "A wide-bandwidth power amplifier for frequency-selective insulator-based dielectrophoresis," *Lab on a Chip*, vol. 14, pp. 4183-4187, 2014.

[3] B. J. Sanghavi, W. Varhue, A. Rohani, K. Liao, L. Bazydlo, C. Chou, N. S. Swami, "Ultrafast immunoassays by coupling dielectrophoretic biomarker enrichment in nanoslit channel with electrochemical detection on graphene," *Lab on a Chip*, vol. 15, pp. 4563-4570, 2015.

[4] A. Rohani, W. Varhue, K. Liao, C. Chou, N. S. Swami, "Nanoslit design for ion conductivity gradient enhanced dielectrophoresis for ultrafast biomarker enrichment in physiological media," *Biomicrofluidics*, vol. 10, pp. 033109, 2016.

[5] P. J. Hesketh, M. A. Gallivan, S. Kumar, C. J. Erdy, and Z. L. Wang, "The application of dielectrophoresis to nanowire sorting and assembly for sensors," Proceedings of the 13th Mediterranean Conference on Control and Automation Limassol, Cyprus, 2005.

[6] B. H. Lapizco-Encinas, R. V. Davalos, B. A. Simmons,E. B. Cummings and Y. Fintschenko, " An insulator-based (electrodeless) dielectrophoretic concentrator for microbes in water," *J. Microbiol. Methods*, vol. 62, pp. 317–326, 2005.

[7] V. Chaurey, A. Rohani, Y. Su, K. Liao , C. Chou, N. S. Swami, "Scaling down constriction-based (electrodeless) dielectrophoresis devices for trapping nanoscale bioparticles in physiological media of high-conductivity," *Electrophoresis*, vol. 34, pp. 49–54, 2013.

[8] G. Fuhr, T. Müller, J. Gimsa, R. Hagedorn, "Traveling-wave dielectrophoresis of microparticles," *Electrophoresis*, vol. 13, pp. 1795-1802, 1992.

[9] A. Rohani, W. Varhue, Y. Su, N. S. Swami, "Electrical tweezer for highly parallelized electrorotation measurements over a wide frequency bandwidth,"*Electrophoresis*, vol. 35, pp. 1795-1802, 2014.

[10] T. B. Jones, Electromechanics of particles (Cambridge University Press, Cambridge, 1995).

[11] H. Morgan and N. G. Green, AC electrokinetics: colloids and nanoparticles. Baldock, Hertfordshire, England. Philadelphia, Pa. Williston, VT: Research Studies Press; Institute of Physics Pub. ; Distribution, North America, AIDC, 2003.

[12] E. Fauss, E. MacCusppie, V. Carver, J. A. Smith, N. S. Swami, "Disinfection action of electrostatic versus steric-stabilized silver nanoparticles on E. Coli,"*Colloids & Surfaces B: Biointerfaces*, vol. 113, pp. 77-84, 2014.

[13] Y. Su, M. Tsegaye, W. Varhue, K. T. Liao, L. Abebe, J. A. Smith, R. L. Guerrant, N. S. Swami,"Quantitative dielectrophoretic tracking for characterization and separation of persistent subpopulations of Cryptosporidium Parvum",*Lab on a Chip*, vol. 14, pp. 4183-4187, 2014.

[14] Y. Su, C. A. Warren, R. L. Guerrant, and N. S. Swami, "Dielectrophoretic Monitoring and Interstrain Separation of Intact Clostridium difficile Based on Their S (Surface)-Layers.", *Anal. Chem.* Vol. 86, pp 10855–10863,2014

[15] A. Rohani, W. Varhue, Y. Su, N. S. Swami, "Quantifying spatio-temporal dynamics of biomarker pre-concentration and depletion in microfluidic systems by intensity threshold analysis,"*Biomicrofluidics*, vol. 8, pp. 052009, 2014.

[16] K. F. Hoettges, "Dielectrophoresis as a cell characterisation tool.", *Methods Mol Biol*. 583:183-98,2010.

 [17] D. J. BAKEWELL, and H.MORGAN,"Quantifying dielectrophoretic collections of submicron particles on microelectrodes." *Meas. Sci. Technol*., 15, 254-266,2004

[18] P, Wagnerova, B. Saka, J. McEvoy, M. Rost, D. Sherwood, K. Holcomb and M. Kvaca, "Cryptosporidium parvum and Enterocytozoon bieneusi in American Mustangs and Chincoteague ponies," *Experimental Parasitology*, vol. 162, pp. 24-27, 2016.

[19] L. Tracey, A. Kirke, P. Armstrong and T. Riley, "From the hospital to the home - The rise and rise of 'Clostridium difficile' infection," *Australian Family Physician*, vol. 44, pp. 712-717, 2015.

[20] W. Wang, T. Ishino, A. Joyce, A. Tam, W. Duan, L. Lin, W. S. Somers and R. Kriz. " Faster in vivo clearance of human embryonic kidney than Chinese hamster ovary cell derived protein: Role of glycan mediated clearance," *J. of Bioscience and Bioengineering*, vol. 119, pp. 657-660, 2015.

[21] B. G. Hawkins, C. Huang, S. Arasanipalai and B. J. Kirby, "Automated dielectrophoretic characterization of mycobacterium smegmatis", *Analytical Chemistry*, vol. 83, pp. 3507–3515, 2011.

[22] J. Regtmeier, R. Eichhorn, M. Viefhues, L. Bogunovic, and D. Anselmetti, "

Electrodeless dielectrophoresis for bioanalysis:Theory, devices and applications.",*Electrophoresis*,Vol32,2253-73,2011

[23] L. M .Broche, K. F. Hoettges, Y. Hübner, S. L. Ogin, G.E. Kass, and M. P.Hughes ,

 "Dielectrophoresis-activated multiwell plate for label-free high-throughput drug assessment."*Anal Chem*. Vol 80 pp 2063-8,2008

 [24] Z. Wissner-Gross , "The Electric field inside a charged ring",www.schoolyourself.org

 [25] Y. Su, A. Rohani, C. A. Warren and N. S. Swami, "Tracking Inhibitory alterations during interstrain clostridium difficile interactions by monitoring cell envelope capacitance", *ACS Infectious Diseases*, accepted, DOI: 10.1021/acsinfecdis.6b00050.